



**HAL**  
open science

# Tracing fluid signature and metal mobility in complex orogens: insights from Pb-Zn mineralization in the Pyrenean Axial Zone

Alexandre Cugerone, Stefano Salvi, Kalin Kouzmanov, Oscar Laurent,  
Bénédicte Cenki

## ► To cite this version:

Alexandre Cugerone, Stefano Salvi, Kalin Kouzmanov, Oscar Laurent, Bénédicte Cenki. Tracing fluid signature and metal mobility in complex orogens: insights from Pb-Zn mineralization in the Pyrenean Axial Zone. *Mineralium Deposita*, In press, 10.1007/s00126-024-01329-5 . hal-04780280

**HAL Id: hal-04780280**

**<https://hal.science/hal-04780280v1>**

Submitted on 18 Nov 2024

**HAL** is a multi-disciplinary open access archive for the deposit and dissemination of scientific research documents, whether they are published or not. The documents may come from teaching and research institutions in France or abroad, or from public or private research centers.

L'archive ouverte pluridisciplinaire **HAL**, est destinée au dépôt et à la diffusion de documents scientifiques de niveau recherche, publiés ou non, émanant des établissements d'enseignement et de recherche français ou étrangers, des laboratoires publics ou privés.



# Tracing fluid signature and metal mobility in complex orogens: insights from Pb-Zn mineralization in the Pyrenean Axial Zone

Alexandre Cugerone<sup>1,2</sup> · Stefano Salvi<sup>3</sup> · Kalin Kouzmanov<sup>2</sup> · Oscar Laurent<sup>3,4</sup> · Bénédicte Cenki<sup>1</sup>

Received: 25 April 2024 / Accepted: 21 October 2024  
© The Author(s) 2024

## Abstract

Orogenic processes encompass a complex interplay of deformation and metamorphic events, which can impact the formation of ore deposits to various degrees. However, distinguishing fluid signatures from orogenic versus post-orogenic events presents a significant challenge due to the scarcity of robust geochemical indicators that remain unaffected during multiple post-mineral reworking events. This study carefully examines the properties and chemistry of primary and secondary fluid inclusions (FIs), identifying distinct signatures of two fluid populations linked to different styles of Pb-Zn mineralization in the Pyrenean Axial Zone (PAZ) of Southern-France/Northern-Iberia: These included late-Carboniferous stratabound epigenetic Pb-Zn deposits and Mesozoic crosscutting Pb-Zn(-Ge) vein systems. Population (I) is identified in primary and secondary FIs in a few crosscutting Pb-Zn veins and constitutes a minor component in stratabound epigenetic bodies. It exhibits Na-dominated low to intermediate salinity (<20 wt% NaCl eq.), intermediate temperatures (200–350 °C), abundant CO<sub>2</sub>-rich FIs and shows low homogeneous Cl/Br molar ratios. These characteristics are consistent with a metamorphic origin of the fluids, associated with Late-Variscan metamorphism. Population (II) is commonly observed in the crosscutting vein systems where it occurs as primary and pseudosecondary FIs, as well as in stratabound epigenetic bodies where it represents the main fluid component of secondary FIs. Population (II) is Ca-dominated with intermediate to high salinity (15–35 wt% NaCl eq.), relatively low temperature (<200 °C), and shows high Cl/Br molar ratios with significant variations. This last characteristic is typical of mixing of at least two fluids, one with a probable low Cl/Br molar ratio at shallow crustal levels and another with high Cl/Br molar ratio at deeper levels. Characteristics of population (II) are consistent with a fluid of basinal origin that interacted with the basement while circulating in the Pyrenees during the Mesozoic, although a Pyrenean-Alpine age cannot be excluded. Locally, in sphalerite-hosted secondary FIs that form trails in the crosscutting veins, we find evidence of high Ge concentrations (up to few 1000s ppm), which correlate with anomalous Pb and Tl concentrations. Very high metal concentrations (up to 1–2 wt% Pb, Zn), which are inversely proportional to Cl/Br molar ratios, are found in FIs mainly within veins hosted in deep-seated high-grade metamorphic rocks. Based on a compilation of fluid data from the literature, a first-order correlation can be deduced between the metamorphic grade of the rocks hosting the mineralization and the Pb and Zn content in the FIs. Early stratabound orebodies are considered likely sources of metal for the development of the late crosscutting vein mineralization. This

Editorial handling: D. Banks

✉ Alexandre Cugerone  
alex.cugerone@gmail.com

Stefano Salvi  
stefano.salvi@get.omp.eu

Kalin Kouzmanov  
kalin.kouzmanov@unige.ch

Oscar Laurent  
oscar.laurent@get.omp.eu

Bénédicte Cenki  
benedicte.cenki@umontpellier.fr

<sup>1</sup> Géosciences Montpellier, Université de Montpellier, CNRS, Montpellier, France

<sup>2</sup> Department of Earth Sciences, University of Geneva, Geneva, Switzerland

<sup>3</sup> Géosciences Environnement Toulouse, Université de Toulouse, CNRS, IRD, OMP Toulouse, France

<sup>4</sup> Institute of Geochemistry and Petrology, ETH Zürich, Zürich, Switzerland

study demonstrates the significance and complexity of orogen-scale fluid circulation and supports the importance of pre-existing metal enrichment in the crust, especially in high-grade metamorphic rocks as a prerequisite for the formation of Pb-Zn veins in complex multi-stage orogens.

### Highlights

- Two fluid populations with distinct fluid inclusion types, salinity, temperatures, Ca-Sr and halogen concentrations.
- Population (I) has a low to medium salinity and high temperature (250–350 °C).
- Population (II) has a medium to high salinity and low temperature (<200 °C).
- The low Cl/Br molar ratios in population (I), along with its Ca-poor and CO<sub>2</sub>-rich characteristics, are indicative of metamorphic fluids.
- The high and variable Cl/Br molar ratios in population (II), along with its Ca-rich and CO<sub>2</sub>-poor characteristics, evidence a major basinal fluid flow.
- Correlation between metamorphic grades, Pb-Zn concentration in fluid and Cl/Br ratio.
- Germanium is locally observed concentrated in Pb-Tl rich sulfosalts phases hosted in FIs trails that intersect deformed sphalerite.

**Keywords** Fluid inclusions · Orogeny · Pb-Zn mineralization · Remobilization · Sulfide · Pyrenean Axial Zone

## Introduction

Orogens are built during a series of tectono-metamorphic events that range from early subduction-collision to late-orogenic extensional as well as post-orogenic stages (Leach and Rowan 1986; Oliver 1986; Rauchenstein-Martinek et al. 2014; Burisch et al. 2022; Song et al. 2023; Bertauts et al. 2024). All these events promote the circulation of many different types of hydrothermal fluids, from high-grade metamorphism to metasomatism and depositing metals in deep to shallow crust. It is thus a challenging task to track the origin of these fluids in polyphased orogens and to link them to a specific tectonic event.

Analyzing paleo-fluids, trapped as mineral-hosted fluid inclusions (FIs), is an approach that is commonly used to untangle fluid signatures and reconstitute tectonic evolution (Wilkinson et al. 2009; Fusswinkel et al. 2013; Burisch et al. 2016b). However, orogens may be extremely complex systems where fluids and minerals are subject to orogenic and post-orogenic modifications related to fluid-rock interaction, rock buffering and superimposed fluid flow (Oliver 1986; Dewaele et al. 2004; Fusswinkel et al. 2017, 2022). Fluid inclusions can suffer from remobilization/re-equilibration during multiple metamorphic events, resulting in data that rarely reflect a fluid's primary signature and make genetic interpretation extremely challenging (e.g., Goldstein 1994; Yardley 2005; Fall and Bodnar 2018). Nonetheless, a number of components that are present in FIs can withstand fluid-rock interactions. An example of these are the halogens chlorine (Cl) and bromine (Br), whose systematic characteristics have served as successful tracers of fluid processes (Walter et al. 1990; Kesler et al. 1995; Fusswinkel et al. 2018; Scharrer et al. 2023). This is particularly evident

in distinguishing between seawater evaporation and halite dissolution in modern analogues of paleo fluid-dominated environments (Kesler et al. 1995; Banks et al. 2000). The Cl/Br ratio has also been instrumental in distinguishing the circulation of metal-depleted basinal brines with high Cl/Br ratios in the upper crust from fluids at deeper crustal levels, which exhibit low Cl/Br ratios and are relatively rich in metals (800–1000 ppm Pb + Zn; Bons et al. 2014). In this scenario, the metal content of the fluid is inversely proportional to its Cl/Br molar ratio, though the precise origin of the metals remains elusive. Nonetheless, several studies have emphasized the role of hot fluid-flow in metamorphic rocks and interaction with minerals in mobilizing base and critical metals (Tomkins 2007; Hammerli et al. 2015; Kunz et al. 2022). While the Cl/Br ratio systematic could be complemented by iodine measurements to better differentiate between basinal and metamorphic fluids, iodine concentration in FIs is challenging to measure and remains insufficiently studied (Fusswinkel et al. 2018; Scharrer et al. 2023).

Mineral deposits are geological objects genetically linked to intense fluid activity, making them ideal case studies for investigating fluid flow in orogenic settings (Bons et al. 2014; Fontboté et al. 2017; Burisch et al. 2022). Ore-forming fluids tend to selectively flow through discontinuities such as faults, shear zones, lithological interfaces, or other zones of weakness in the Earth's crust. A frequently observed and extensively documented mineral deposit type within orogenic terranes, consists of crosscutting veins containing substantial reserves of lead and zinc (Laznicka 2006; Wilkinson 2013; Müller and Ehle 2021; Luo et al. 2022). In western European terranes, such epigenetic deposits are frequently related to extensional Mesozoic events (Mucchez et al. 2005; Guilcher et al. 2021; Burisch et al. 2022). Probably

the most significant European occurrence of Pb-Zn cross-cutting vein deposits is within the Southern-France/Northern-Iberia district (Fig. 1A), with resources of about 10 Mt of Zn and Pb (Leach et al. 2006). Nevertheless, the origin of the mineralizing fluids forming these Pb-Zn veins and the timing of their circulation remain unclear. This controversy has sparked a debate, giving rise to two potential scenarios: fluid flow and mineralization occurring either during periods of extension or during periods of shortening (Muechez et

al. 2005; Leach et al. 2006; Cathelineau et al. 2021; Burisch et al. 2022; Giorno et al. 2022; Song et al. 2023; Bertauts et al. 2024).

In the core of the Southern-France/Northern-Iberia district (Fig. 1A and B), the Pyrenean Axial Zone (PAZ) is a typical example of a belt that has recorded two major orogenic periods, separated by Mesozoic rifting. The first event is related to the Variscan orogeny (Carboniferous-Permian), while the second took place during the Alpine orogenic

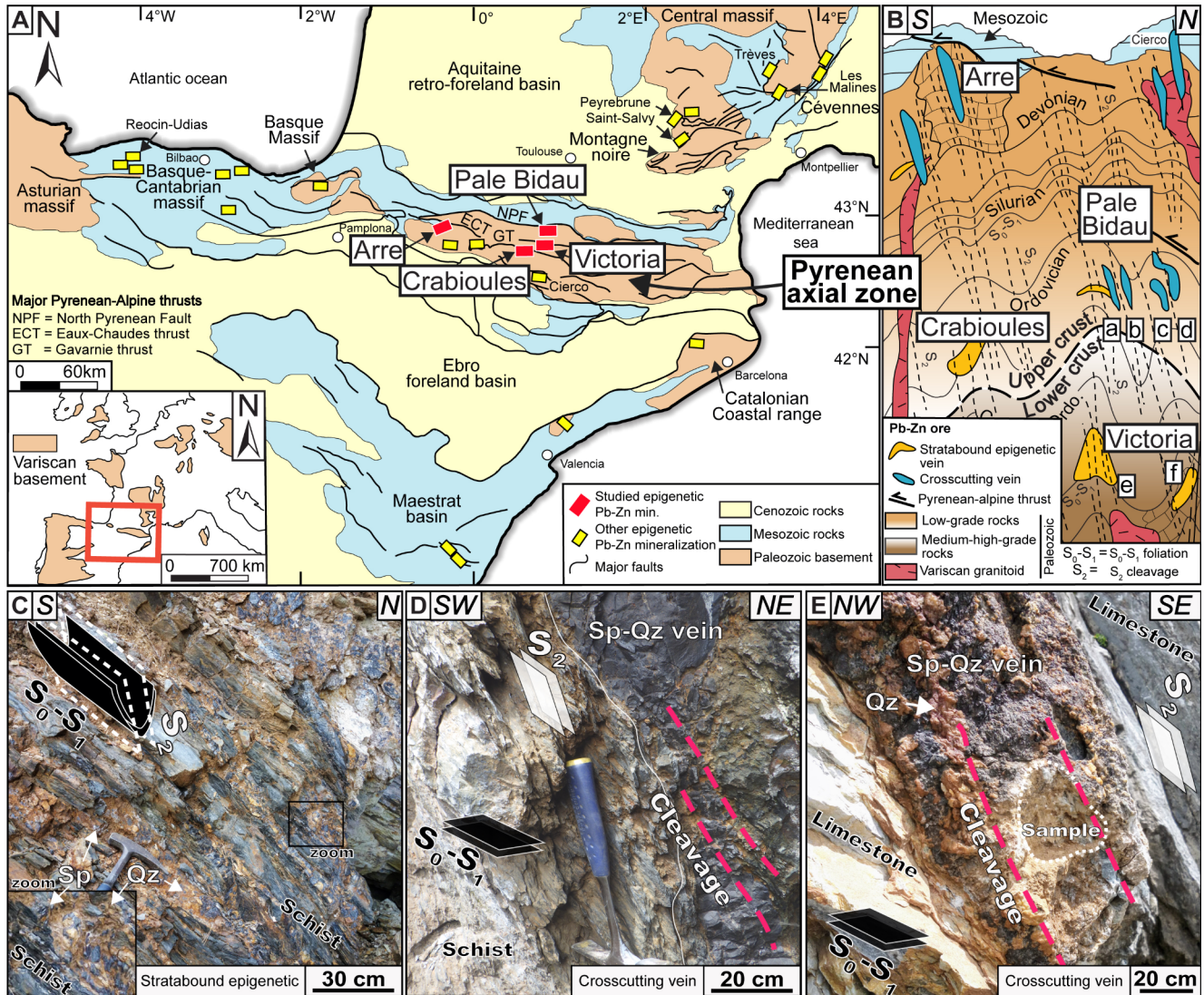


**Fig. 1** A. Simplified structural map of the Pyrenean chain in Western Europe, hosting the Southern-France/Northern-Iberia Pb-Zn district, stretching from the Atlantic Ocean to the Mediterranean Sea (spatial data from BRGM [http://infoterre.brgm.fr] and IGME institutes [http://mapas.igme.es/Servicios/default.aspx]). The deposits studied are shown in red. An inset locates the area shown in A in Europe; B. A schematic, hypothetical N-S section through the Pyrenean Axial zone, illustrating the structural position of the stratabound epigenetic and crosscutting vein deposits (not to scale). For Victoria and Pale Bidau districts, multiple orebodies are identified by a letter referring to: *Pale Bidau district*: a-Pale Bidau vein 1; b-Pale Bidau vein 2; c-Argut-des-

sus; d-Pale de Rase; *Victoria district*: e-Victoria mine; f-Margalida; C. Outcrop photograph of stratabound epigenetic Pb-Zn mineralization in the Victoria mine. Mineralization is hosted in high-grade metamorphic schists (andalusite, staurolite, gahnite), is generally sub-parallel to  $S_0$ - $S_1$  foliation and folded by  $F_2$  upright to isoclinal folds, with sub-vertical  $S_2$  superimposed on mineralization; D-E. Two Pyrenean vein systems crosscutting  $S_0$ -Variscan  $S_1$  foliation and parallel to Variscan  $S_2$  cleavage. The superimposed cleavage observed in sphalerite is newly interpreted as Alpine in age. In (D), sphalerite quartz vein from the Pale Bidau deposit is hosted in low grade metamorphic schists. In (E), sphalerite quartz vein from the Arre deposit is hosted in limestone



period (Late-Cretaceous-Miocene) (Zwart 1979; Vergés et al. 2002). In the PAZ, Pb-Zn mineralization shows evidence of complex multistage formation (Reyx 1973; Pouit and Bois 1986; Johnson et al. 1996; Cugerone et al. 2018b, 2021a, 2024). A first mineralization stage consists of stratabound epigenetic veins that were emplaced and deformed during the Variscan orogeny (i.e., Late-Carboniferous U-Pb age on monazite; Bentaillou stratabound Pb-Zn deposit; Cugerone et al. 2022). These orebodies consist of replacement veins that are structurally and lithologically controlled, exhibiting evidence of secondary remobilization, characterized by saddle-reef textures recurring in the cores of folds (Fig. 1C; Cugerone et al. 2018b). A second mineralization stage comprises epigenetic crosscutting veins (Fig. 1D and E) that, in addition to Pb and Zn, are enriched in critical metals such as Ge and Ga (Castroviejo Bolibar and Serrano 1983; Johnson et al. 1996; Cugerone et al. 2018b, 2020). These undated vein systems may locally intersect the earlier formed stratabound orebodies (Cugerone et al. 2018b).

In this study, we employ microthermometric and LA-ICP-MS data from FI assemblages in several stratabound and vein orebodies from the PAZ to identify two distinctive episodes of fluid flow, each characterized by specific metamorphic and basinal fluid signatures. We compare our findings with published data on similar mineralization types worldwide to develop a genetic model for these two major epochs of fluid circulation. Additionally, we discuss the significance of these fluid-flow episodes in the formation of Pb-Zn deposits.

## Analytical methods

Eight representative samples from the seven deposits studied were prepared (cf. details about the deposits studied below). They were sampled in the main mineralized systems of each deposit, and systematically contain sphalerite and/or galena. The eight samples selected were prepared as doubly polished Sect. (150  $\mu\text{m}$ -thick) to carry out detailed FI petrography using a standard microscope as well as hot cathodoluminescence (CL). Fluid inclusion assemblages (FIA) were defined according to Goldstein and Reynolds (1994) and primary and secondary origin were identified using the criteria of Roedder (1984). Cathodoluminescence (CL) imaging was performed using a HC6-LM hot cathode system by Lumic Special Microscopes at the Géosciences Environment Toulouse (GET) laboratory at 14 kV and a current density of ca. 10  $\mu\text{A mm}^2$  (Neuser 1995). Cathodoluminescence images were captured with a very-high sensitivity Olympus XC10 camera.

Microthermometric measurements were performed at the GET laboratory, according to the procedures outlined

by Roedder (1984), using a Linkam THMGS 600 heating–freezing stage mounted on a BX-51 Olympus microscope. The stage was calibrated using synthetic pure H<sub>2</sub>O FIs (0° and 374.1 °C) supplied by SynFlinch and natural pure CO<sub>2</sub> inclusions (−56.6 °C) from Camperio (Ticino, Switzerland). The accuracy of measurements is  $\pm 0.2$  °C below  $\sim 0^\circ\text{C}$  and  $\pm 1$  °C above 0 °C. Homogenization temperatures were measured at 1 to 5 °C/min heating rates, depending on the inclusion size. Cryogenic experiments were carried out before heating to reduce the risk of decrepitating the inclusions. Melting temperatures of ice, hydrohalite and eutectic estimations (respectively,  $T_{\text{MICE}}$ ,  $T_{\text{MH}}$  and  $T_{\text{FIRST}^-_{\text{M}}}$ ) in FIs were repeated during several runs for accuracy. Fluid salinity data, expressed as wt% NaCl eq. or wt% CaCl<sub>2</sub> eq., were calculated for aqueous FIs using the H<sub>2</sub>O-NaCl (Steele-MacInnis et al. 2011) and H<sub>2</sub>O-NaCl-CaCl<sub>2</sub> (Steele-MacInnis et al. 2012) spreadsheets for aqueous FIs and the H<sub>2</sub>O-NaCl-CO<sub>2</sub> spreadsheet of Steele-MacInnis (2018) for CO<sub>2</sub>-bearing FIs.

LA-ICP-MS analyses were carried out to quantify major, minor and trace element concentrations of FIAs. These analyses were performed at ETH Zurich using the ETH-prototype GeoLas system equipped with a 193 nm ArF-Excimer Compex 102 F laser ablation system (Lamba Physik-Coherent, Germany) coupled to a Nexion2000 (PerkinElmer, USA/Canada) fast-scanning quadrupole ICP-MS for multi-element analysis. Five sample chips were analyzed in a ca. 5 cm<sup>3</sup> round glass cell. Gas blanks and system contamination were minimized following the cleaning and setup procedures proposed by Schlöglova et al. (2017). The cell was fluxed with carrier gas consisting of high-purity (5.0 grade) He (1.1 L min<sup>−1</sup>). Sample gas consisting of 6.0 grade Ar (ca. 1 L min<sup>−1</sup>) was admixed downstream of the ablation cell prior to injection in the plasma. The ICP-MS was optimized for maximum sensitivity on the entire mass range and low oxide rate formation (<sup>248</sup>ThO+/<sup>232</sup>Th + < 0.5%). The contents of Na and Cl were calculated based on microthermometric results. In order not to overestimate the Na content with respect to Cl, and to provide a balance between cations and anions, the sum of total cations was subtracted from the value of Na. Chlorine contents were calculated by subtracting the total salinity obtained from microthermometry from the calculated Na contents. The amount of Cl associated with Ca in the form of CaCl<sub>2</sub> (based on Ca content from LA-ICP-MS measurements) was added to total calculated Cl content. The glass standard NIST SRM 610 (Jochum et al. 2011) was used as a primary reference material except for Br. The Sca-17 scapolite standard (Seo et al. 2011) was used as the primary reference material for Br (ESM1). Both standards were analyzed with 40  $\mu\text{m}$  pit size, repetition rates of 10 Hz and energy densities of ca. 5 J.cm<sup>−2</sup>, during ca. 1 min measurement consisting of 30 s gas blank + 30 s

ablation. Fluid inclusions in quartz were analyzed by slowly incrementing the spot size using an opening aperture (“iris diaphragm”) to prevent cracking (Guillong and Heinrich 2007). Laser repetition rates of 10 Hz and energy density on sample of ca. 10 J.cm<sup>-2</sup> were applied. Sphalerite was analyzed with a laser repetition rate of 5 Hz and energy density of ca. 9 J.cm<sup>-2</sup>. In total, 35 elements were measured with a dwell time of 5 ms for <sup>7</sup>Li, <sup>11</sup>B, <sup>23</sup>Na, <sup>25</sup>Mg, <sup>29</sup>Si, <sup>39</sup>K, <sup>55</sup>Mn, <sup>85</sup>Rb, <sup>88</sup>Sr, <sup>93</sup>Nb, <sup>133</sup>Cs, <sup>138</sup>Ba, <sup>140</sup>Ce, <sup>203</sup>Tl, <sup>208</sup>Pb, <sup>74</sup>Ge, <sup>232</sup>Th, <sup>238</sup>U, 10 ms for <sup>34</sup>S, <sup>35</sup>Cl, <sup>43</sup>Ca, <sup>57</sup>Fe, <sup>63</sup>Cu, <sup>66</sup>Zn, <sup>75</sup>As, <sup>107</sup>Ag, <sup>111</sup>Cd, <sup>115</sup>In, <sup>121</sup>Sb and 20 ms for <sup>78</sup>Br. The elements Mg, Nb, Ce, Th, U, S, As, and In were not detected in the FIs. The total sweep time was 180 ms. Data were reduced with the SILLS software (Guillong et al. 2008), using the salinity determined by microthermometry as internal standard for the FIs and stoichiometric contents of major elements as internal standard to correct the contribution of the host mineral (Si for quartz and Zn-Fe for sphalerite).

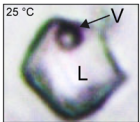
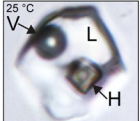
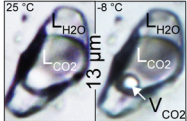
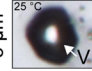
## Sampling strategy and characterization

Stratabound epigenetic Pb-Zn orebodies were sampled in the Victoria district, including Victoria mine and Margalida mine, and in the Crabioules district (Figs. 1B and C and 2). These form structurally and lithologically controlled replacement veins hosted in lower-crustal levels (Fig. 1B and C). In Victoria, Ordovician high-grade metamorphic schist (andalusite, staurolite) host the mineralization, with local Zn-rich gahnite observed (Cugerone et al. 2018b). In Margalida, mineralization is hosted in highly deformed marble, in the damaged zone of the regional Bossòst fault (García-Sansegundo and Alonso 1989; Cochelin et al. 2017), and in Crabioules, Pb-Zn mineralization is hosted in muscovite-biotite Ordovician schist (Pouit 1985; Cugerone

et al. 2018b). No significant hydrothermal alteration is observed around the orebodies. Sphalerite and galena frequently occur as millimetric polygonal crystals, a texture suggesting static recrystallization with widespread presence of annealing twins and low amount of intra-granular ductile deformation (Cugerone et al. 2024). Locally, sphalerite shows lobate textures and is more concentrated in the core of folds (saddle-reef) related to Variscan orogeny, which was interpreted to represent remobilization during Variscan stages (Fig. 3Cugerone et al. 2022). Quartz is frequently fractured and displays evidence of recrystallization with bulge nucleation (Fig. 3A-C). Minor occurrences of pyrrhotite and chalcopyrite are found in these two deposits with a notable absence of Ge-minerals.

Epigenetic crosscutting Pb-Zn veins were sampled at the Pale Bidau (Pale Bidau mine, Pale de Rase and Argut-dessus mine) and at the Arre districts (Figs. 1D and E and 2). These veins are subvertical and are interpreted to post-date the stratabound Pb-Zn orebodies. They share a similar mineralogy and sphalerite texture with the sub-vertical veins that crosscut stratabound orebodies in the Liat deposit, Central Pyrenees (Cugerone et al. 2018b, 2022). In the Pale Bidau and Arre districts, the vein mineralogy mostly consist of quartz, sphalerite, galena, pyrite, barite and graphite. At Pale Bidau, the vein system is generally parallel to the Variscan E-W S<sub>2</sub> cleavage and hosted in upper-crustal levels consisting of Late-Ordovician muscovite calc-schists, conglomerate and marbles (Fig. 1B and D) (Cugerone et al. 2018a). The Arre vein district is hosted in upper-crustal levels composed of Devonian low-grade metamorphic limestone. In these veins, quartz is not significantly recrystallized and is locally fractured (Fig. 3D-F). The main sulfide mineral observed in these crosscutting veins is sphalerite, which postdates quartz (Fig. 3D). Sphalerite shows a highly heterogeneous texture and chemistry, largely affected by

**Fig. 2** Major characteristics of quartz-hosted fluid inclusion (FIs) types from the studied deposits. All the photomicrographs are taken at room temperature (T°= 25 °C) except the L-L<sub>CO2</sub> FIs with visible V<sub>CO2</sub> taken at T°= - 8 °C

Fluid inclusion type	Photomicrograph	Phases at room T°	Petrographic position	Type of host quartz	Deposit	Population
A - aqueous inclusions L-V <sub>H2O</sub>		H <sub>2</sub> O Liquid (L) Vapor (V)	Secondary (fractures)	Stratabound epigenetic	Margalida	(I)
			(Pseudo)-secondary (fractures)	Crosscutting vein	Argut-dessus	(I)
			Primary (growth zones)		Arre Pale Bidau Pale de Rase	(II) (I) (II) (I)
B - brine inclusions L-V-H		H <sub>2</sub> O Liquid (L) Vapor (V) Halite (H)	Secondary (fractures)	Stratabound epigenetic	Victoria Crabioules	(II) (II)
			C - aqueous-carbonic inclusions L-L <sub>CO2</sub>		H <sub>2</sub> O Liquid (L) CO <sub>2</sub> Liquid (L)	Secondary (fractures)
Primary (growth zones)	Crosscutting vein	Argut-dessus				(I)
(Pseudo)-secondary (fractures)		Pale Bidau				(I)
D - vapor-rich inclusions V		Vapor (V)	Secondary (fractures)	Stratabound epigenetic	Victoria Crabioules	(II) (II)
			Primary (growth zones)	Crosscutting vein	Arre	(II)
			Secondary (fractures)			



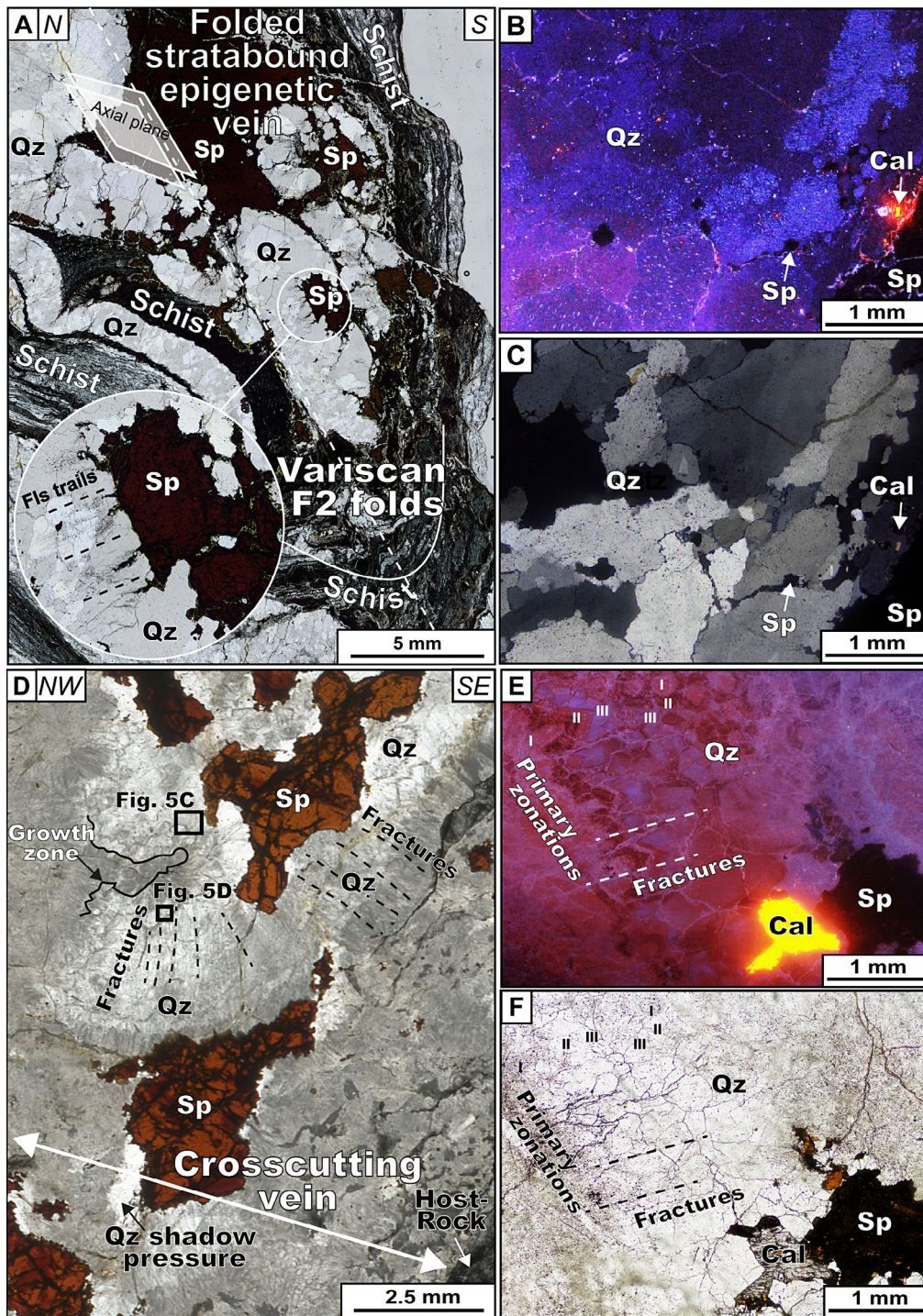


**Fig. 3** Microphotographs of the studied samples in transmitted plane polarized light and in cathodoluminescence (CL). Sections used for cathodoluminescence and FIs analyses are from the same sample but in different thick sections (Abbreviations: Cal: calcite; Qz: quartz; Sp: spherulite): **A**. Folded (Variscan F2 folds) spherulite and quartz stratabound veins hosted in gahnite-schist from Victoria. Note the FIs trails close to the dislocated spherulite bodies in the F2 fold hinge; **B–C**. Cathodoluminescence and transmitted cross polarized light photos with early deformed quartz compared to spherulite in stratabound mineralization from Victoria. Note in (**B**), the non-uniform tints of blue in quartz grains, opaque black color for spherulite and orange color

for a small crystal of calcite on the right; **D**. Crosscutting vein from Arre with spherulite and quartz. Note the presence of late fractures crosscutting growth zones in quartz. These two textures host primary and secondary FIs, respectively. Spherulite is also intensely fractured with local presence of FIs. **E–F**. Cathodoluminescence and transmitted cross polarized light photos showing textural relationships between quartz, calcite and spherulite at Arre. Growth zones in different quartz generations (I, II, III) differ by cathodoluminescence colors with tints of dark red to blue. Spherulite shows an opaque black color with cathodoluminescence and is late compared to quartz

dynamic recrystallization. Coarse grains shows wide color variations from dark- to light-brownish domains in plane polarized transmitted light (Cugerone et al. 2020). Compared to quartz, sphalerite has a “ductile” behavior and recrystallizes at relative low temperature (200–300 °C; cf., Cugerone et al. 2024). The light-brown regions in this mineral commonly show evidence of recrystallization with neo-formation of small pluri-micrometric crystals. The dark brown zones were only observed in the coarse parental grains and are enriched in Ge, Cu, and Ga (i.e., Cugerone et al. 2021a). This contrasts with the light sphalerite domains, which are significantly depleted in these elements (i.e.; < 100 ppm Ge; Cugerone et al. 2021). Ge-minerals such as briartite ( $\text{GeCu}_2(\text{Fe}, \text{Zn})\text{S}_4$ ) are observed at the micro- and nanoscale (Fougerouse et al. 2023).

In the Pale Bidau, Pale de Rase and Argut-dessus cross-cutting veins, quartz systematically precipitates prior to sphalerite. At Pale de Rase, quartz exhibits comparatively limited fracturing in contrast to the Pale Bidau and Argut-dessus quartz. In these three crosscutting vein systems, sphalerite is essentially fine-grained, almost entirely recrystallized, and has low Ge, Ga and Cu contents (i.e., < 20 ppm Ge). In contrast to the sphalerite found in the Arre veins, this sulfide recorded significant variations in Fe content (up to 2–4 wt% Fe), resulting in millimeter-size chemical zoning, visible as light- to dark-brown bands that are unrelated to grain boundaries (Cugerone et al. 2018a). In addition, Ge-minerals such as brunogeierite ( $\text{GeFe}_2\text{O}_4$ ) and argutite ( $\text{GeO}_2$ ) are found along sphalerite grain boundaries. They are commonly grouped in the more porous domain hosted in the main schistosity, which corresponds to the Variscan  $\text{S}_2$  cleavage (Cugerone et al. 2021a, 2024).

## Results

### Fluid inclusion petrography and microthermometry

From the four districts studied, quartz grains were selected in close association with sphalerite. In quartz from stratabound epigenetic Pb-Zn orebodies (Victoria and Crabioules districts), only secondary FIs assemblages (FIAs) were identified (Figs. 2 and 3A). Specifically, quartz from the Victoria mine is commonly observed with secondary FIs trails next to the sphalerite aggregates (Figs. 3A and 4). In crosscutting veins from Pale Bidau and Arre districts, quartz shows abundant growth zones containing primary and pseudosecondary FIAs, as well as sealed fractures containing secondary FIAs (Figs. 2, 3D and 5A–D). A total of 383 individual FIs, grouped in 68 FIAs, were analyzed in quartz from eight samples from the four districts studied (the full dataset is provided in the ESM1).

In addition to quartz, FIs were also studied in sphalerite. However, FIs-bearing sphalerite crystals were only found at Arre (36 individual FIs in 7 FIAs). Here, sphalerite is composed of coarse parental grains and small recrystallized grains. FIAs occur exclusively in the dark domains of the parental grains where they mostly consist of single inclusions aligned in fractures. The light domains, whether coarse or recrystallized crystals, are systematically devoid of FIs (Fig. 5E and F). Despite multiple efforts, microscopic observations in coarse grains, both in visible and near infrared light, did not allow for proper identification of the phases present in the sphalerite-hosted FIs, as most of them remained opaque. It is considered that the opacity of FIs in sphalerite is due to the negative crystal shape of the inclusion vacuoles (Bonev and Kouzmanov 2002), which prevents the light to exit the FIs.

Based on petrography and microthermometry, we distinguished four types of FIs in quartz (Figs. 2, 4 and 5): (A) aqueous liquid-vapor FIs ( $\text{L-V}_{\text{H}_2\text{O}}$ ) are < 40  $\mu\text{m}$  in size and contain 10 to 15 vol% vapor. These were found in all cross-cutting vein sites within primary to pseudosecondary FIAs, and in stratabound epigenetic orebodies only as secondary FIAs (Crabioules and Victoria; Fig. 2); (B) Liquid-vapor-halite FIs ( $\text{L-V-H}$ ) measure up to 60  $\mu\text{m}$  in diameter and contain 10 to 15 vol% vapor and a small halite crystal occupying 5 to 10 vol% of the inclusion volume. This type was only identified as secondary FIAs in quartz from stratabound epigenetic orebodies (Fig. 5A–C); (C) Aqueous-carbonic liquid-liquid FIs ( $\text{L-L}_{\text{CO}_2}$ ) measure up to 40  $\mu\text{m}$  and contain variable amounts of  $\text{CO}_2$  (20–80 vol%, optical microscopy). In quartz from stratabound epigenetic orebodies (Crabioules and Victoria district), these FIs form either secondary trails associated with  $\text{L-V-H}$  FIs or pluri-millimetric isolated clusters (Fig. 5A–D). In crosscutting veins from Pale Bidau and Argut-dessus mines,  $\text{L-L}_{\text{CO}_2}$  FIs are pseudosecondary in origin, and are associated with  $\text{L-V}_{\text{H}_2\text{O}}$  FIs (Fig. 5A and B), but in the Arre crosscutting veins, no  $\text{L-L}_{\text{CO}_2}$  FIs were observed (Fig. 5C and D); (D) Vapor-rich inclusions (V) measure up to  $\sim 15 \mu\text{m}$  and are of primary origin in the Arre cross-cutting veins. Similar inclusions were also observed in the stratabound epigenetic orebodies, where they are secondary in nature (Fig. 5C).

Microthermometric runs evidenced two compositional populations (Fig. 6), both of which observed in the stratabound epigenetic as well as in the crosscutting vein orebodies (Fig. 6). Population (I) was found as primary to pseudosecondary FIAs from Pale Bidau veins and secondary FIAs from the Victoria district (Victoria mine and Margalida; Fig. 6A). It consists of aqueous ( $\text{L-V}_{\text{H}_2\text{O}}$ ) or aqueous-carbonic ( $\text{L-L}_{\text{CO}_2}$ ) FIs of low to intermediate salinity ( $\sim 1$ –18 wt% NaCl eq.). High  $\text{Th}_{\text{CO}_2}$  (from 0 to 20 °C) were found in  $\text{L-L}_{\text{CO}_2}$  FIs from Victoria, Crabioules and



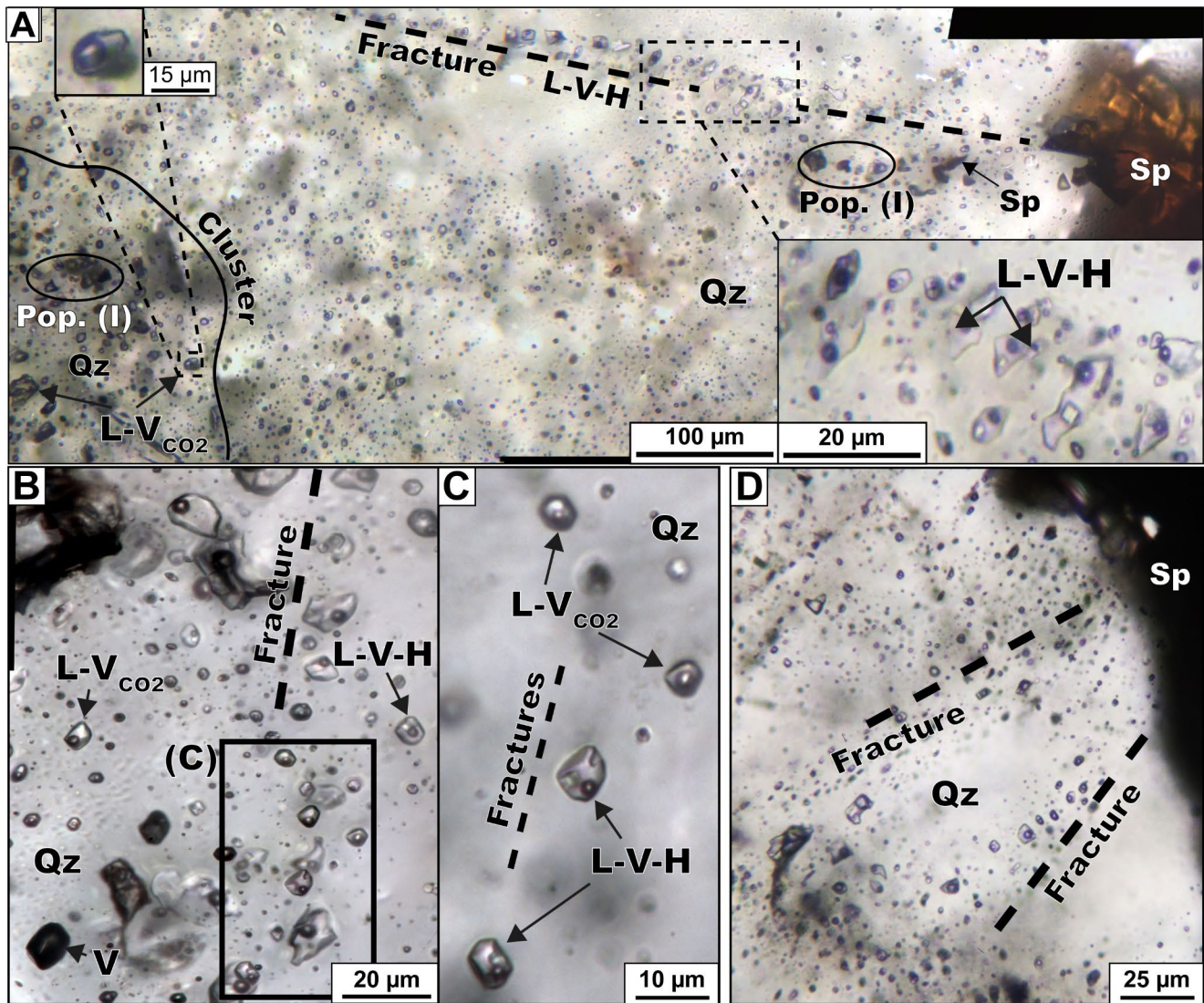


**Fig. 4** Petrography of FIs in quartz from stratabound epigenetic mineralization (Abbreviations: Qz: quartz; Sp: sphalerite). All photomicrographs are taken in transmitted light: **A**. Secondary L-V-H FIs in secondary trails with small halite crystals and local clusters of L-V<sub>CO2</sub> FIs (Victoria (a), focus stacking); **B-C**. Secondary L-V-H FIs associ-

ated with L-V<sub>CO2</sub> FIs in fractures (Crabioules; focus stacking). Zoom in (C) with no focus stacking shows association of L-V-H and L-V<sub>CO2</sub> FIs; **D**. Secondary FIs with association of L-V-H and L-V<sub>CO2</sub> FIs in trails close to sphalerite (Margalida; focus stacking)

Pale Bidau districts associated with L-V<sub>H2O</sub>, whereas low Th<sub>CO2</sub> (from -45 to -30 °C) occur in clusters of L-L<sub>CO2</sub> FIs in Victoria and Crabioules, isolated from L-V<sub>H2O</sub> or L-V-H FIs (Figs. 4A and 6B). Aqueous (L-V<sub>H2O</sub>) and aqueous-carbonic (L-L<sub>CO2</sub>) FIs have Th<sub>H2O</sub> and Th<sub>TOT</sub> reaching moderate to high temperatures, respectively (200–350 °C; Fig. 6A and B). Population (II) is trapped as primary and secondary FIs in Arre veins, in secondary FIs in a Pale Bidau vein, and in secondary FIs in the Crabioules and Victoria stratabound epigenetic orebodies (Figs. 4, 5 and 6). It consists of aqueous (L-V<sub>H2O</sub>), aqueous with halite (L-V-H) of moderate to high salinity (10–32 wt% NaCl eq.). Minor aqueous-carbonic (L-L<sub>CO2</sub>) FIs were locally found associated with

L-V-H FIs in the Victoria and Crabioules districts within the same FIs trails (Fig. 4C) and show high Th<sub>CO2</sub> (from 0 to 20 °C). Only in this population (II), up to 6–13 wt% CaCl<sub>2</sub> eq. is reported, indicative of compositions belonging to the H<sub>2</sub>O-NaCl-CaCl<sub>2</sub> system. Homogenization temperatures of L-V<sub>H2O</sub> FIs are moderate (Th<sub>AQ</sub> = 150–250 °C; Fig. 6A).

#### Fluid composition and halogen concentrations

In quartz and sphalerite, 230 individual FIs grouped in 91 FIAs were analyzed by LA-ICP-MS to obtain compositional information (full dataset is reported in ESM1). These results confirm the existence of two populations as already



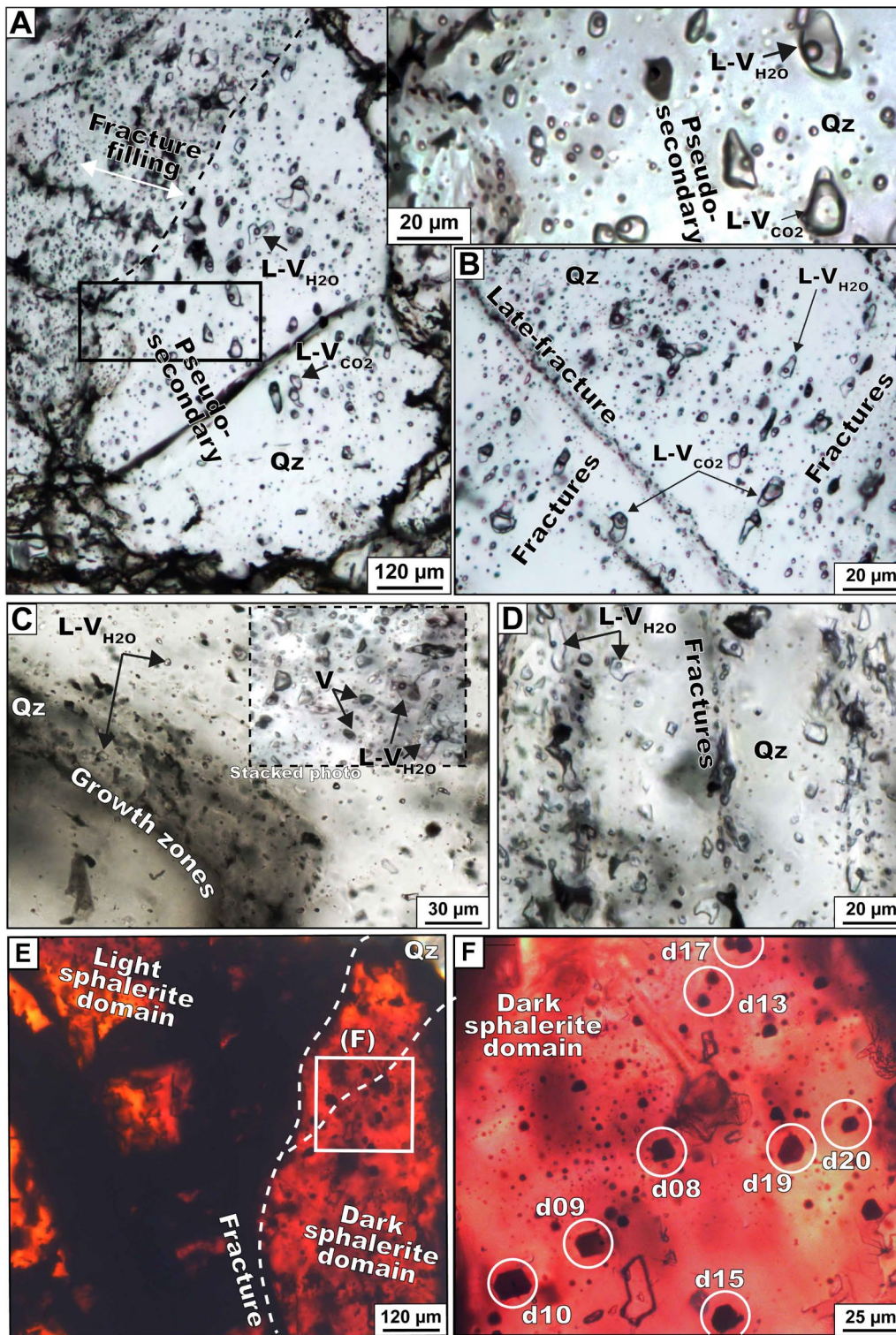


**Fig. 5** Petrography of FIs in quartz (A–D) and in sphalerite (E–F) from crosscutting vein mineralization (Abbreviations: Qz: quartz; Sp: sphalerite). **A.** L-V<sub>H2O</sub> FIs filling fracture or occurring as pseudo-secondary FIs associated with L-L<sub>CO2</sub> FIs (Pale Bidau, focus stacking); **B.** Primary L-V<sub>H2O</sub> FIs associated with L-V<sub>CO2</sub> FIs in growth zones. Minor L-V FIs are hosted in late-fractures (Argut-dessus; focus stacking); **C.**

Primary L-V<sub>H2O</sub> FIs associated with V FIs in growth zones (Arre); **D.** Secondary L-V<sub>H2O</sub> FIs aligned along fractures (Arre; stacked image). **E.** Dark and light domains in sphalerite with local late fracture (Arre). **F.** Zoom in sphalerite from area in (E), showing secondary FIs. Location of LA-ICP-MS spots is mentioned and each LA-ICP-MS spot names are reported in ESM1

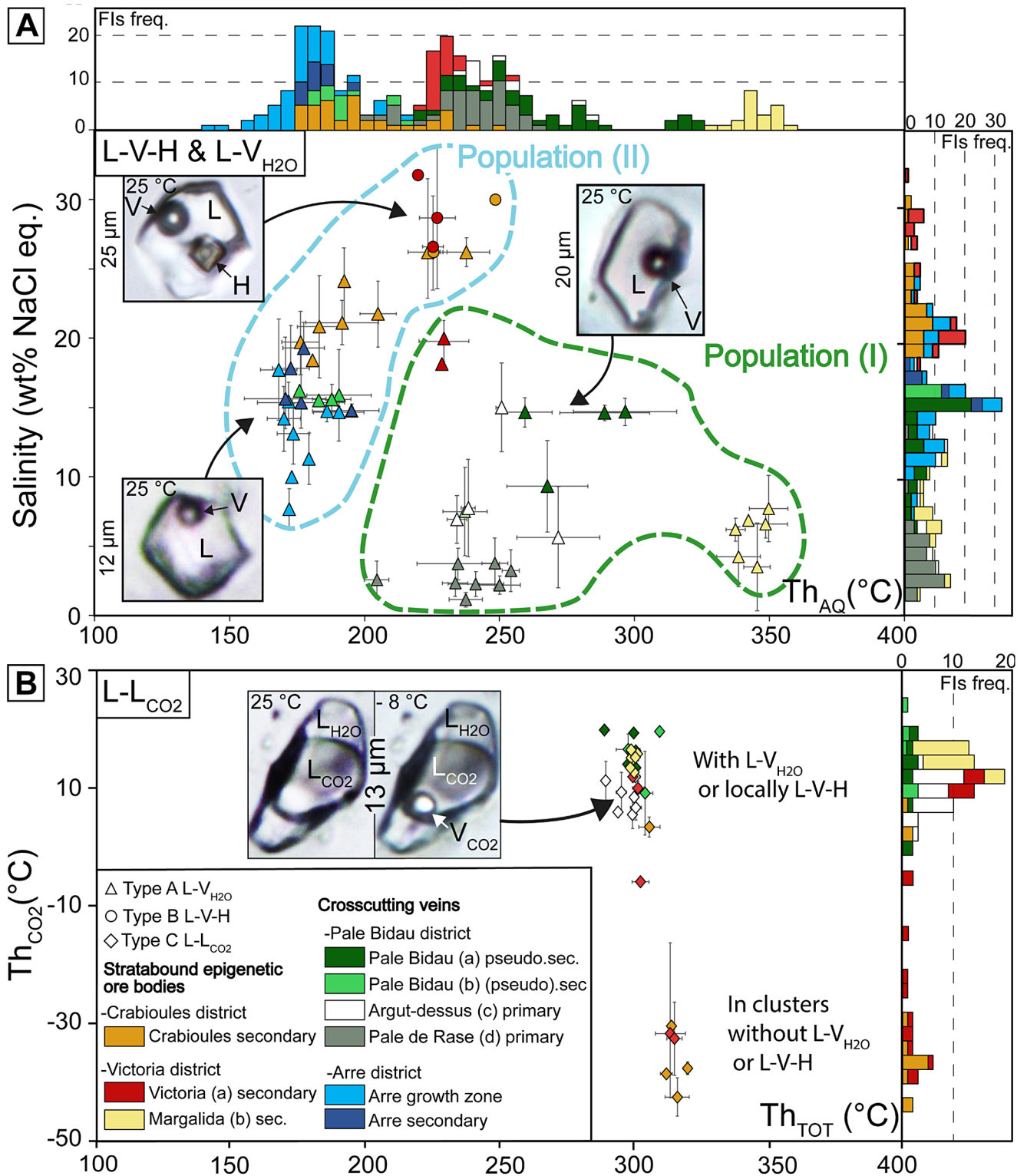


**Fig. 6** Fluid inclusion microthermometric data obtained in quartz from stratabound epigenetic and crosscutting vein orebodies. Frequency histograms are also shown; A. Salinity vs. homogenization tempera-

ture for L-V-H and L-V<sub>H2O</sub> FIAs. a FIA; B CO<sub>2</sub> homogenization temperature vs. total homogenization (°C) for L-L<sub>CO2</sub> FIAs



deduced based on microthermometric data. Population (I) is systematically depleted in Ca compared to population (II) (Figs. 7 and 8A). The two populations also differ in Sr and Ba contents, defining two distinct trends marked mostly by higher Ba values for the former (Fig. 8B). Both populations showed extremely high Pb and Zn contents in some cases (up to 1 and 2 wt%, respectively; Figs. 7 and 8C). The laser ablation time-integrated signals (Fig. 8A–B) shows that Pb and Zn peaks are slightly displaced compared to the main Na and Cl peaks, which appear upon FIs breach. This pattern is indicative of the presence of nano to micro-sized solid inclusions that are ablated slightly after the fluid is vaporized. In both FIs populations, Pb and Zn concentrations follow roughly a 1:1 mass ratio in all localities studied (Fig. 8C). In the one sphalerite crystals where FIs could be measured (at Arre), the inclusions locally exhibited remarkably high Ge concentrations, reaching up to few thousands of ppm Ge. In the time-integrated LA-ICP-MS signals, Ge spikes were systematically observed in the FIs intervals where high Ge values may or may not correlate with other metals (Pb, Tl; Fig. 7C–D).

Halogen data exhibit distinct signatures for populations (I) and (II). In Fig. 8D, normalized using Na and Cl values, population (I) shows low Cl/Br ( $52 \pm 34$ ) and Na/Br ( $51 \pm 34$ ; nFIAs=9) molar ratios close to the 1:1 line. Population (II) lies between the 1:1 and 10:1 lines, indicating Na loss related to significant Ca-rich FIs. Population (II) has high and variable Cl/Br ( $216 \pm 200$ ) and Na/Br ( $178 \pm 174$ ) molar ratios, with an upper Na–Cl–Br trend close to seawater composition (nFIAs=45). Some data present large 1 sigma errors for the concentrations of metals, Cl and Br, possibly due to heterogeneous entrapment and presence of tiny solids in the FIs (Fig. 8D–E), which were not identified optically.

## Discussion

### Two distinct fluid populations in pyrenean Pb–Zn deposits

The findings from the FIs study, particularly the patterns defined by FIs types (CO<sub>2</sub>-rich, halite-rich), salinity, homogenization temperatures, Ca–Sr–Ba concentrations and halogen concentrations underscore the existence of two FIs populations, occurring in both stratabound and cross-cutting vein orebodies. This clearly implies the involvement of distinct fluid types in the genesis of these deposits. Fluid inclusion population (I) shows medium to high temperatures (200–350 °C), is rich in CO<sub>2</sub>, has low salinity (NaCl + CaCl<sub>2</sub>), low Sr/Ba ratio and low homogeneous Cl/Br molar ratio (Figs. 6 and 8). Population (II) is indicative of a low- to medium-temperature brine (<250 °C)

characterized by intermediate to high NaCl–CaCl<sub>2</sub> contents, high Sr/Ba ratio and high Cl/Br molar ratio with significant variations (14–2000). Our results suggest that the fluid represented by population (I) was the main mineralizing fluid at Pale Bidau, Argut-dessus, Pale de Rase, while the fluid represented by population (II) was responsible for depositing the ore at Arre (Figs. 6 and 8). This can be deduced from the fact that the two types of fluids were found in primary FIs, respectively in each of these deposits. However, in stratabound epigenetic orebodies, exemplified by the case of the Victoria, Margalida and Crabioules, we could not detect any primary FIA and both fluid types were detected only in FIAs of secondary origin (Figs. 6, 8 and 10A).

An enrichment in Ca and Sr in fluid (II) was not only found in samples from the marble-hosted deposit at Arre, but also at Crabioules and Victoria, which are hosted in schist. This infers that the Ca–Sr enrichment cannot be simply related to interaction of the fluid with the host rock, and that this signature is likely a regional mark, probably due to fluid flow within carbonate units at a regional scale (Fig. 8A and B). Both fluids have been shown to be enriched in metals (mainly Pb, Zn, Mn), however but they cannot be discriminated based only on their Pb and Zn concentrations (Fig. 8C). For FIs hosted in quartz at Arre (fluid II), microthermometry and LA-ICP-MS data indicate similar NaCl–CaCl<sub>2</sub>, Ca–Sr, and metal concentrations whether the FIs are hosted in growth zones (i.e., primary) or in fractures (i.e., secondary) (Fig. 9). At Arre, sphalerite postdates quartz (Fig. 3D), but the same fluid composition was found in FIs from both minerals, implying that a similar fluid system was active during the formation of quartz and sphalerite and continued during deformation of the latter. Presence of necking-down or any other evidence implying post-entrapment equilibration were not observed. Therefore, we interpret the similarity between the chemistry of primary and secondary FIs at Arre as indicative of comparable fluid-flow conditions and compositions from deposition to deformation.

### Tracing fluid origin using halogen signatures

Identifying diagnostic geochemical indicators, such as the Cl/Br signature, enrichment in Na or Ca enrichment or the presence of CO<sub>2</sub>-rich FIs, is particularly useful for determining the origin of a fluid (i.e., metamorphic, basinal fluids) in complex orogenic systems. The Cl/Br molar ratio of population (I) is relatively homogeneous, suggesting the presence of only one type of fluid. The low Cl/Br trend (Fig. 8D) is not consistent with a seawater or halite dissolution origin (Channer et al. 1997; Fusswinkel et al. 2022). Such low Cl/Br molar ratio might be associated with repeated interactions between a fluid and the host-rock, as may occur during fluid flow through fine-grained infill in



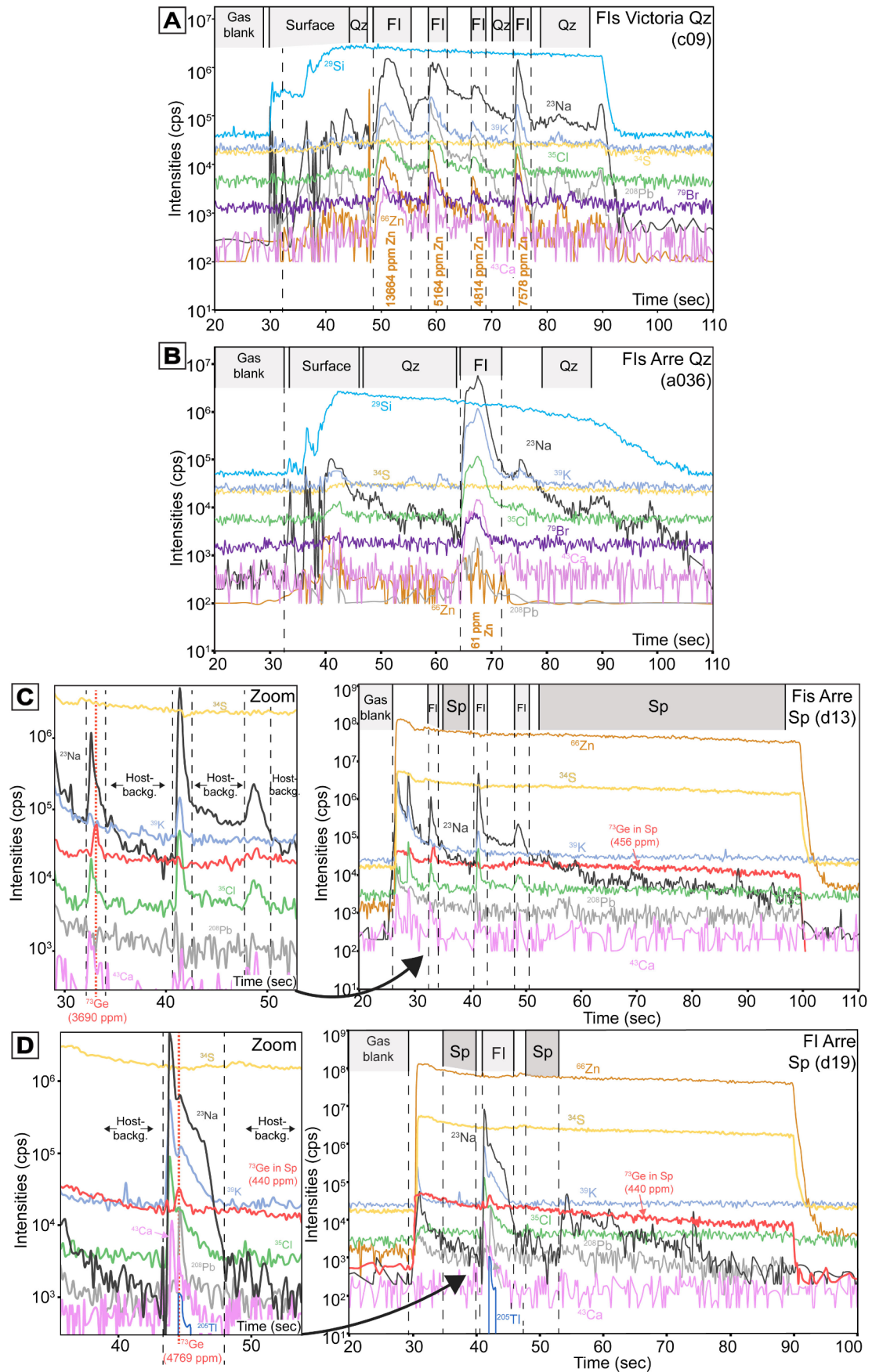


**Fig. 7** Time-integrated LA-ICP-MS signals for selected elements in quartz (A-B) and sphalerite (C-D). Concentrations in Zn are indicated for each quartz-hosted inclusion. **A.** Four FIs in stratabound epigenetic mineralization from the Victoria mine. **B.** One FI in crosscutting vein from the Arre deposit; **C.** Three FIs in crosscutting vein from the Arre deposit. **D.** One FI in crosscutting vein from the Arre deposit

cataclastic fractures (Burisch et al. 2016a). Alternatively, it could represent an influence on the fluid from Br-enriched organic matter during metamorphism (Miron et al. 2013; Fusswinkel et al. 2017, 2018, 2022; Scharrer et al. 2023). If the former is an unlikely scenario given the settings of the deposits, sedimentary sequences in the PAZ commonly do contain abundant organic matter. For instance, in the Pale Bidau deposit, abundant graphite is found associated with sulfides (Cugerone et al. 2018b) and in Victoria, graphite is locally present in sphalerite-quartz vein. A compilation of FIs LA-ICP-MS data from metamorphic terranes in various settings and basinal fluids (Fig. 10B) shows significant variations in the Na-Cl-Br signature, generally following the 1:1 line. This shows that the low Cl/Br signature related to Br enrichment is not, alone, a diagnostic indicator of a metamorphic fluid origin because a similar Br enrichment could occur in residual evaporitic brines (Fusswinkel et al. 2022; Scharrer et al. 2023), which in our dataset is also confirmed by the presence of local Br-rich FIs in population (II) (i.e., data with low Cl/Br and Na/Br values from Arre FIs; Fig. 8D and E). In the case where iodine measurements are not available as an additional constraint, other geochemical indicators become necessary (Scharrer et al. 2023). One such indicator is the fact that metamorphic fluids are generally Na dominated and commonly induce entrapment of CO<sub>2</sub>-rich FIs (Yardley and Bodnar 2014; Yardley and Cleverley 2015). In contrast, basinal fluids often show a significant Ca enrichment and lower amounts of dissolved CO<sub>2</sub> (Bons et al. 2014). In our samples, population (I) is Na-dominated and frequently contains CO<sub>2</sub>-rich FIs, which, together with a low Cl/Br molar ratio, is strongly indicative of a metamorphic origin. Such fluid may have percolated through various organic-rich rocks, such as regional Silurian black-schist levels which are typically enriched in graphite, and formed most of the vertical veins in the Pale Bidau district. Although geochronological data are currently not available for these veins, no evidence for metamorphism has been reported in the literature for the PAZ during the Pyrenean-Alpine orogeny, with the possible exception for local Early-Cretaceous Mg metasomatism that only exhibits a Cl/Br molar signature typical of basinal fluids (100–500 Cl/Br molar ratio; Quesnel et al. 2019; Fig. 10B). It is thus reasonable to suggest that fluid population (I) was related to the main Variscan metamorphic period that affected the PAZ (Zwart 1963; Mezger and Passchier 2003) during the Early-Permian.

On the other hand, the Cl/Br vs. Na/Br trend of population (II) is typically Ca-rich (trend between 1:1 and 10:1) and is offset to the lower left from the SW reference in Fig. 8D, which is indicative of evaporation or other Br-enriching processes such as residual evaporitic fluids (Kesler et al. 1995; Bons et al. 2014). Such huge Cl/Br compositional range (14–2000; Fig. 11) implies the presence of both a residual brine and a halite dissolution brine component that underwent mixing processes, and certainly cannot be due to a single fluid type. Halite dissolution may have been inherited during fluid percolation in basement lithologies, such as Triassic evaporitic levels of regional extent (Figs. 8D and 9A and B; Cathelineau et al. 2021). Comparing our results from population (II) as well as those from published studies of another Pyrenean Pb-Zn vein deposit (Johnson et al. 1996) and compilation of data from fluids trapped in syn-orogenic Alpine quartz (Banks et al. 1991; McCaig et al. 2000), reveals striking similarities in salinity, temperature, Na-Ca composition and Cl/Br signatures (Figs. 8D-E and 9A). Plotting Cl/Br vs. Na/Br data from the Southern-France/Northern-Iberia district as well as from the extensively studied carbonate-hosted deposits in the US and the Schwarzwald district in Germany, reveals several similarities in trends (Fig. 10B). This compilation shows broadly comparable Cl/Br vs. Na/Br trends in late-Paleozoic to Mesozoic veins of several carbonate-hosted deposits in the US and the Schwarzwald district, as well as to several Pb-Zn districts in Spain (Maestrat and Basque-Cantabrian basins; Grandia et al. 2003a, b), syn-rift Early-Cretaceous metasomatism in the Pyrenees (Quesnel et al. 2019), and in the Cévennes basement in the Southern French Massif Central (Leach et al. 2006). These trends are generally typical of basinal fluids and aligns with the signature of population (II), which supports the hypothesis that these mineralizing fluids originated from basinal fluids that interacted with basement rocks (i.e., Fig. 10B). While the absence of geochronological data precludes speculation on the precise timing of mineralization (Fig. 9B), resemblances in fluid composition between primary FIs in quartz growth zones at Arre and secondary FIs in fractures related to late-Alpine shear zones (Fig. 9B), including the presence of a Ca-rich system, poor content in L-LCO<sub>2</sub> FIs and similar metal and halogen concentrations, could suggest an Alpine-related origin for population (II) and the corresponding crosscutting veins (Fig. 10B). Nonetheless, circulation of mineralized brines interacting with the basement (unconformity type; Bons et al. 2014) during widespread rifting events of Mesozoic age at Arre and similar vein systems cannot be excluded (e.g., Johnson et al. 1996).

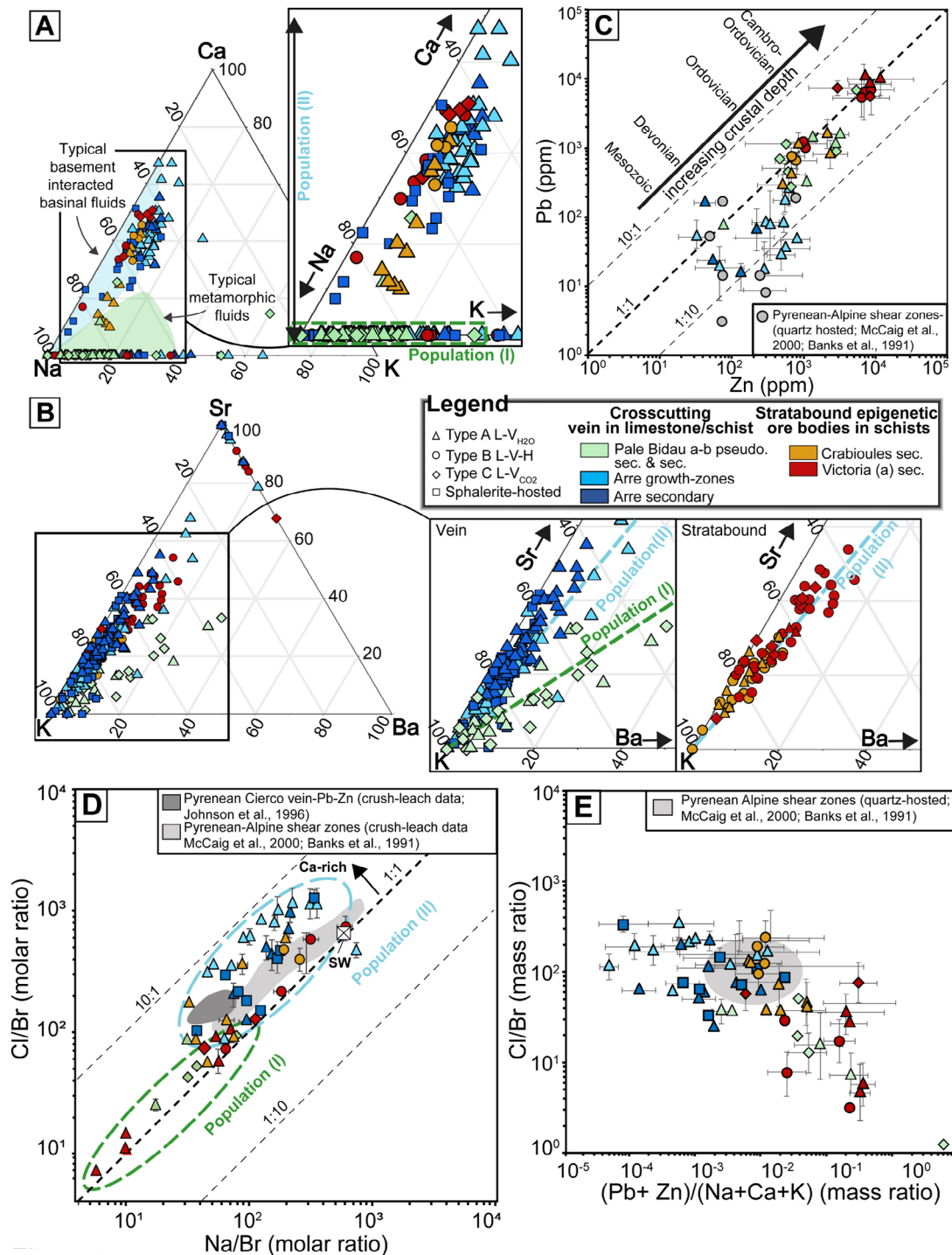


**Fig. 8** **A.** Relative proportions of Na-Ca-K for individual FIAs; data are presented as mass concentrations. Date references: metamorphic fluid field: Marsala et al. 2013; Miron et al. 2013; Rauchenstein-Martinek et al. 2014, 2016; Fusswinkel et al. 2022; basinal fluids that interacted with basement rocks in Pb-Zn rich deposits: Heijlen et al. 2008; Stoffell et al. 2008; Wilkinson et al. 2009; Appold and Wenz 2011; Bouhrel et al. 2016; Mu et al. 2021; **B.** Relative proportions of K-Sr-Ba for individual FIAs; data are presented as mass concentrations. **C.** Diagram plotting Pb vs. Zn concentrations in all FIAs (FIAs in sphalerite are not considered because of host-contamination for Zn). Published

data for the Pyrenees (grey circles), with crush-leach data acquired in the Pyrenean-Alpine shear zones (Banks et al. 1991; McCaig et al. 2000) are also shown for comparison; **D.** Cl/Br vs. Na/Br (molar ratio) systematic for all FIAs from our study. Published data from Pyrenean shear zones (Banks et al. 1991; McCaig et al. 2000) and Cierco Pb-Zn deposit (Johnson et al. 1996) are also shown; **E.** Cl/Br vs. (Pb + Zn + Mn)/(Na + Ca + K) (mass ratio) diagram for all FIAs, with data from the Pyrenean-Alpine shear zones in gray for comparison (Banks et al. 1991; McCaig et al. 2000)

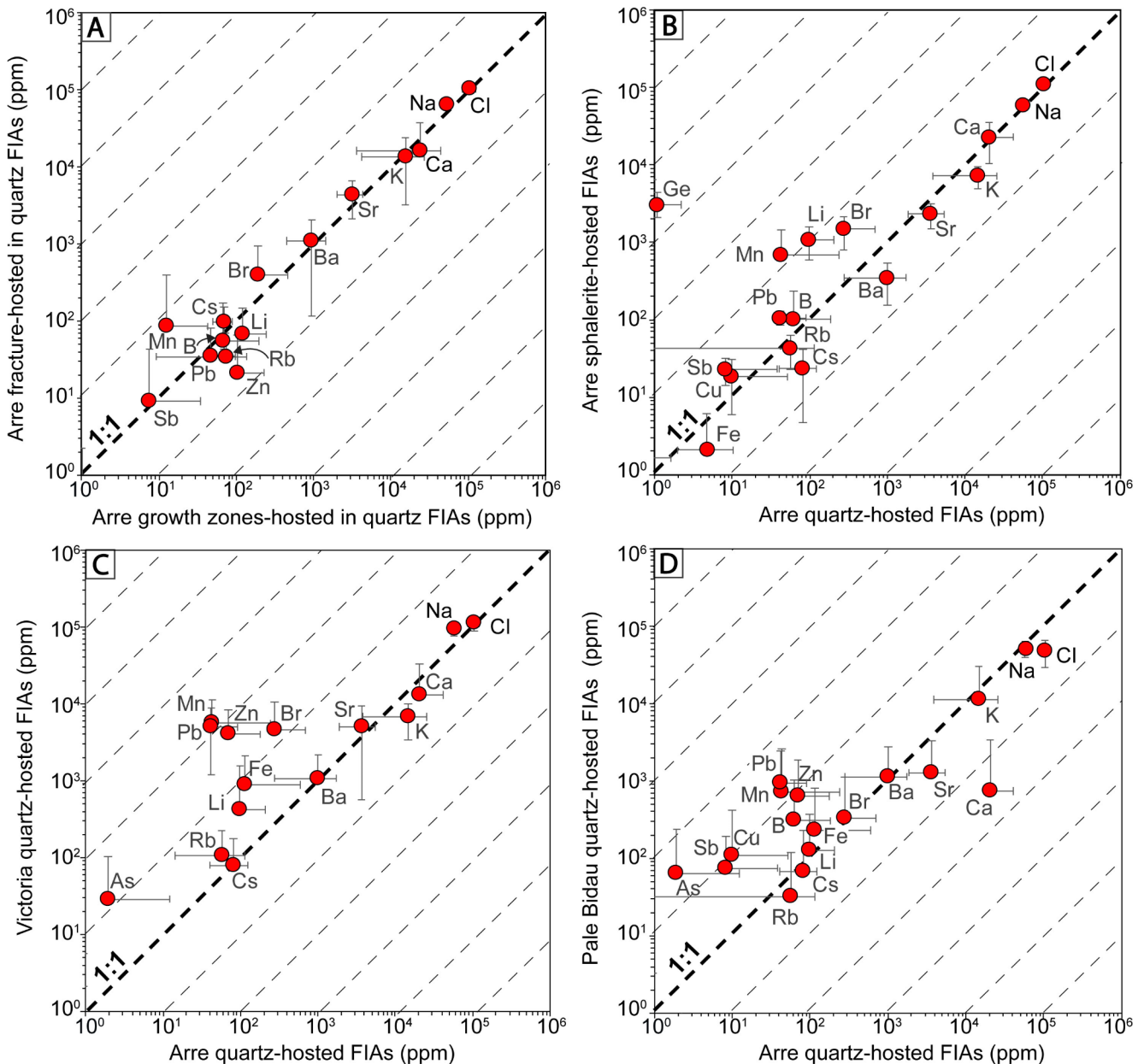


**Fig. 9** Comparison of element concentration data from FIAs between: **A.** FIAs in growth zones and fractures in Arre quartz (vein); **B.** FIAs in sphalerite and quartz in Arre (vein); **C.** FIAs in Victoria (stratabound) and Arre (vein) quartz; **D.** FIAs in Pale Bidau and Arre quartz (vein)

### Lead, zinc and germanium mobility in orogenic and post-orogenic systems

Fluid inclusion studies, when coupled with detailed structural analysis, offer a valuable tool for tracking fluid-assisted metal mobility in orogenic systems. By analyzing the composition and characteristics of FIAs, it becomes possible to gain valuable insights into the nature of fluids that flowed through the system and on the mechanisms driving metal mobilization at different stages of tectonic activity. In the sphalerite sample from the Arre deposit, population

(II) fluids are trapped as secondary FIAs in dark domains of coarse parental sphalerite grains. Comparing data from quartz- and sphalerite-hosted FIAs shows higher Ge, Mn, Pb, Li, and Sb concentrations in inclusions from sphalerite, values that are not due to contamination from the FIAs host. Noteworthy, the occurrence of isolated, small correlated Ge-Pb-Cl-K-(-Tl) spikes in the LA-ICP-MS signals are likely due to the presence of Ge-rich sulfosalt crystals that precipitated inside the FIAs (Fig. 7C and D), rather than indicating high amounts of Ge, Pb and Tl in solution as suggested by Sośnicka et al. (2023) in a study of Zn-Pb



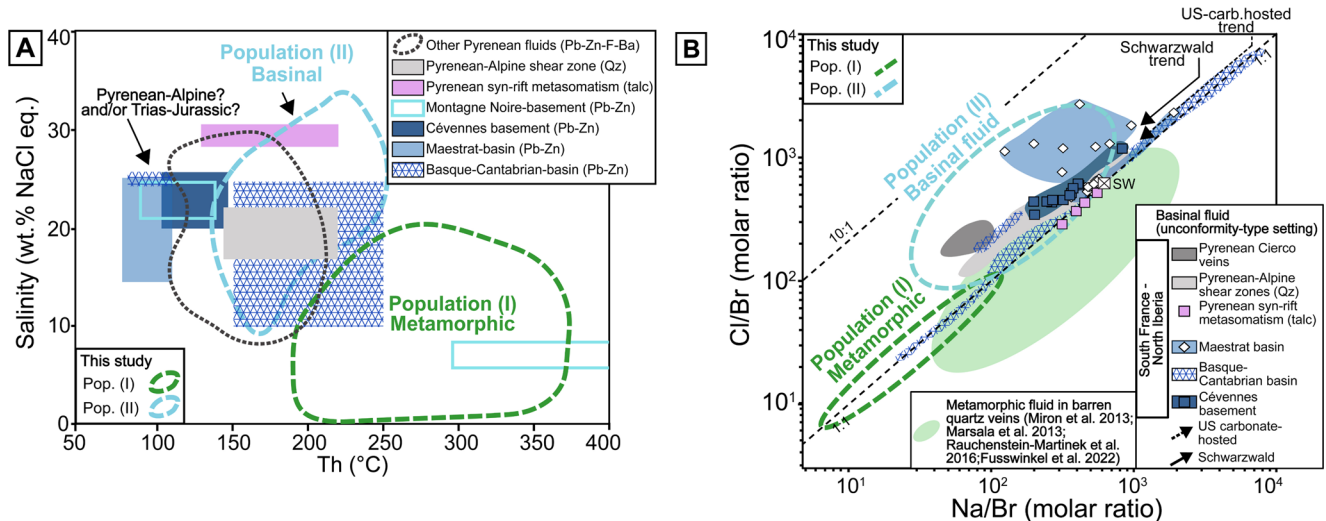


**Fig. 10** **A.** Compilation of microthermometry data from the Southern-France/Northern-Iberia district from the literature and this study. *Data references:* Banks et al. 1991; Muñoz et al. 1994, 1997, 2016; Johnson et al. 1996; Fanlo et al. 1998; Subias et al. 1999; McCaig et al. 2000; Grandia et al. 2003a, b; Leach et al. 2006; **B.** Literature compilation for Cl/Br systematics including LA-ICP-MS and crush-leach data for basinal fluids that interacted with basement rocks and quartz veins related to metamorphic fluids (field with light green color). Data from

this study are also plotted with trends illustrated by dashed dark-green and blue lines. The low Cl-/Br signature related to Br enrichment is not, alone, a diagnostic indicator of a metamorphic fluid origin. *Data references:* Banks et al. 1991; Johnson et al. 1996; McCaig et al. 2000; Grandia et al. 2003a, b; Leach et al. 2006; Stoffell et al. 2008; Wilkinson et al. 2009; Fusswinkel et al. 2013, 2022; Marsala et al. 2013; Miron et al. 2013; Rauchenstein-Martinek et al. 2016; Quesnel et al. 2019; Scharrer et al. 2023

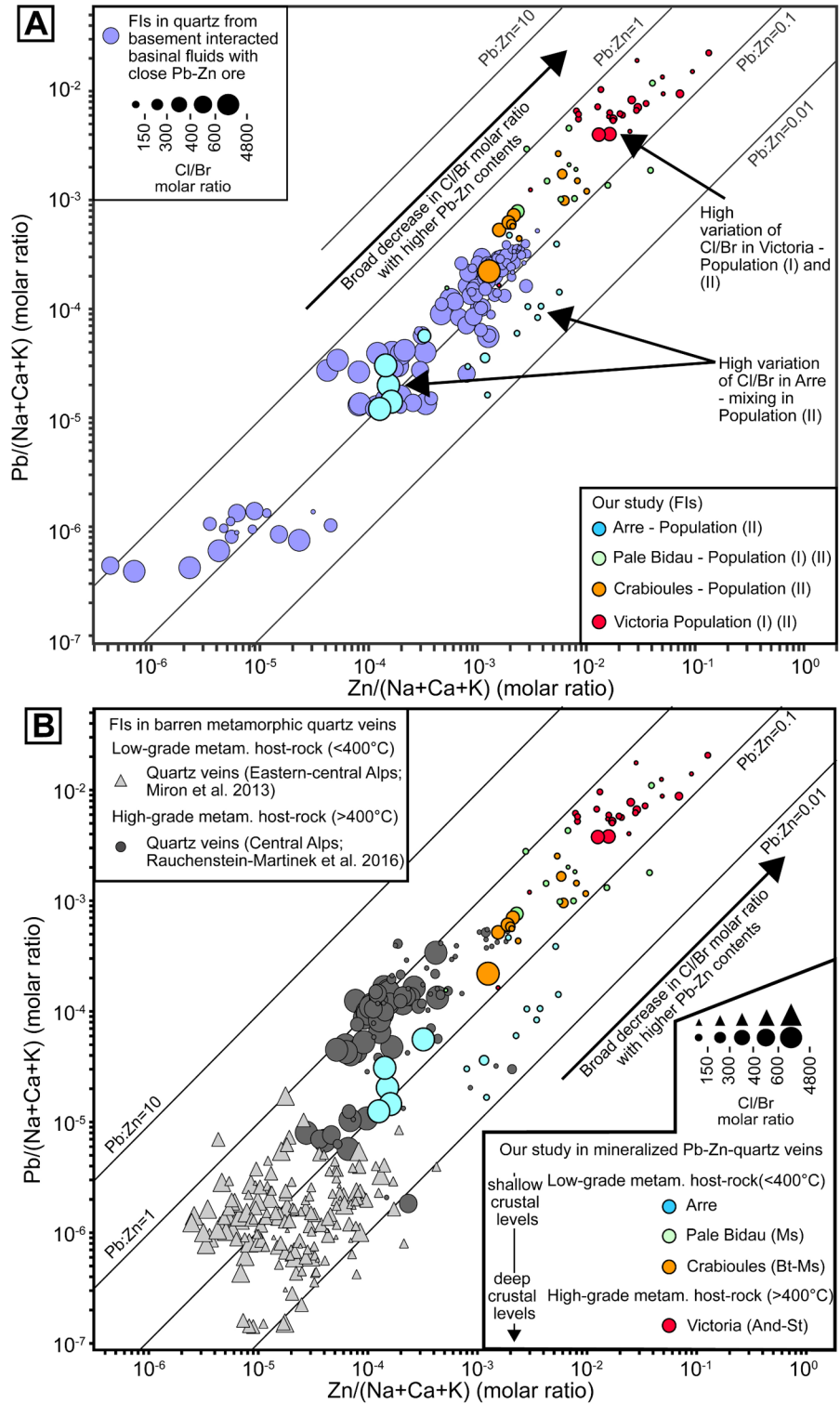
mineralization from the North German basin. Albeit a correlation is reported between Ge and Pb in Cu-poor colloform sphalerite (Luo et al. 2022; Sun et al. 2023), their chemical behavior in a fluid and incorporation mechanisms in sphalerite are not well understood. The sporadic occurrence of Ge-rich sulfosalts only in secondary FIs that are hosted in healed fractures crosscutting deformed sphalerite supports local, fluid-assisted remobilization of Ge. This probably occurred shortly after the redistribution of Ge in sphalerite which only caused the formation of Ge-Cu sulfides (briartite; Fougere et al. 2023). Additional Ge input from an external source is not considered plausible because of the systematically low Ge concentrations (mostly < LOD) measured in quartz-hosted primary and secondary FIs from the same samples. Moreover, while these micro-fractures have been documented as being parallel to a Variscan cleavage trend in sphalerite, their age is undoubtedly Alpine rather than Late-Variscan as previously suggested. This conclusion arises from the implication of a Mesozoic to Alpine age for vein emplacement, as clearly evidenced, for instance, at Arre (Cugerone et al. 2021a).

A compilation of LA-ICP-MS data from FIs providing metal contents (Pb, Zn; obtained by salinity normalization using Na + Ca + K) in basinal fluids that interacted with the basement (Fig. 11A) and from metamorphic quartz veins in various settings (Fig. 11B) shows a similar Pb-Zn correlation with molar ratios ranging from 1:1 to 1:100. The Cl/Br molar ratios, represented by the size of circle or triangle

symbols in Fig. 11A and B, are clearly inversely proportional to the metal content (Pb, Zn) in the fluids, excluding local variations related to fluid mixing.

In the Arre veins, which contain FIs population (II), metal concentrations (Pb, Zn) are relatively low (mostly < 100 ppm; Fig. 8C). These veins are hosted in very low-grade metamorphic rocks (limestone) and were emplaced at upper crustal levels (Fig. 1B). In carbonate-hosted deposits formed by low-temperature basinal fluids that interacted with basement rocks (< 250 °C), such as the Irish Pb-Zn deposits or some MVT deposits in the United States, Pb and Zn have similar concentrations (up to few 100s ppm) in quartz-hosted FIs (Yardley 2005; Stoffell et al. 2008; Wilkinson et al. 2009). Such low concentrations are interpreted to be related to the significant uptake of metals from the fluid by precipitating sulfides (sphalerite, galena; Stoffell et al. 2008; Wilkinson et al. 2009). In contrast, in the Victoria, Crabioules and Pale Bidau deposits, secondary FIs (Fig. 4; Cugerone et al. 2018b) of the population (I) and (II) are significantly enriched in metals, probably in the form of micro to nanoscale Pb-Zn solid phases, imparting concentrations up to 1–2 wt% Pb and Zn to the fluid (Figs. 8C and 11A). These stratabound and crosscutting veins are hosted in moderate- to high-grade metamorphic rocks (up to andalusite-staurolite stability), which are indicative of deep crustal levels (Fig. 1B). Data from barren metamorphic quartz veins reported in the literature (Fig. 11B) indicate a similar depth/metamorphic grade dependency of metal tenor,

**Fig. 11** Compilation of Pb and Zn trace element data (LA-ICP-MS) from FIs in the literature compared with the data from this study (see ESM1 for full dataset). The Pb and Zn data are normalized with Na + Ca + K and presented in molar contents. **A.** Comparison between data from this study and data from unconformity-type deposits with close Pb-Zn ore. Data are generally included between the ratio Pb: Zn = 1 and Pb: Zn = 0.01. Data from Arre show similar Pb-Zn contents compared to other unconformity-type deposits (Schwarzwald) but Victoria, Pale Bidau and Crabioules show higher Pb and Zn contents. *Dataset references:* McCaig et al. 2000; Heijlen et al. 2008; Stoffell et al. 2008; Fusswinkel et al. 2013; Bouhlef et al. 2016; Mu et al. 2021; **B.** Comparison between metamorphic barren quartz vein and quartz vein close to Pb-Zn ore from our study. Fluid in barren quartz veins hosted in high-grade metamorphic rocks (> 400 °C) show higher Pb-Zn contents compared to barren quartz vein hosted in low grade metamorphic rocks (< 400 °C). Similarly, fluid from Victoria quartz veins hosted in high-grade metamorphic rocks show higher Pb and Zn content compared to Arre, Crabioules and Pale Bidau hosted in low grade metamorphic rocks. *Dataset references:* Miron et al. 2013; Rauchenstein-Martinek et al. 2016



with barren quartz veins in high-grade metamorphic rocks typically containing higher metal concentrations. However, metal concentrations in barren quartz veins from high-grade metamorphic setting also correlate with those found in low-grade veins from Arre. This discrepancy could be attributed to differences in metal stock between barren and

mineralized Pb-Zn veins, with higher Pb-Zn concentrations in fluids from veins located near Pb-Zn mineralization.

In population (II), the variations in Cl/Br molar ratio (not observed in population (I) combined with metal concentrations in the fluid (Figs. 11 and 12), may reflect changes in mixing ratios between a deeper brine rich in metals and Br

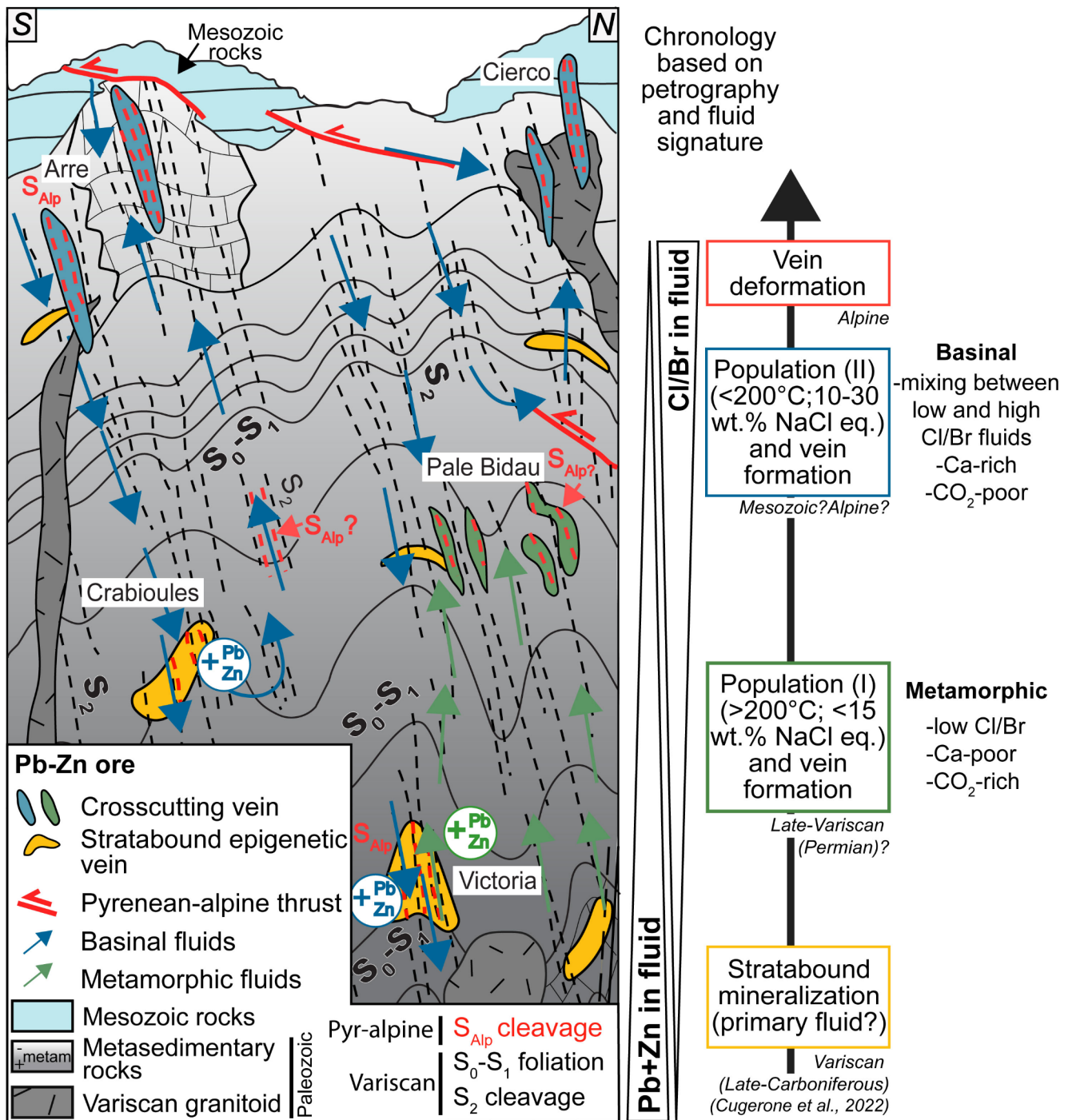


**Fig. 12** Schematic cross-section based on Fig. 1B through the Pyrenean axial zone (PAZ) representing the two main fluid populations reported in this study. Location of the studied deposits is indicated as well as Cierco (Johnson et al. 1996). The main Paleozoic and Mesozoic lithologies are represented with superimposed deformation structures

(thrust,  $S_0$ - $S_1$  foliation,  $S_2$  cleavage). On the right, general variations in Pb-Zn and Cl/Br ratio in fluid at crustal scale are represented. A relative timescale indicates the characteristics of the two fluid populations and their proposed chronology

and a shallower halite-dissolution brine depleted in metals and Br. This situation is very similar to that observed in the Schwarzwald area (Bons et al. 2014). As a result, a first-order correlation can be inferred between the depth of emplacement/metamorphic grade of the host-rock, the enrichment in Pb and Zn and the Cl/Br molar ratio measured from FIs (Fig. 12). This relationship can be further influenced by the quantity of metal deposited within sulfide minerals in the veins.

In FIs from magmatic-hydrothermal systems, it is common to observe metal concentrations higher than 1 wt%. However, such environments are characterized by much higher temperatures than those of the present study (e.g., Landtwing et al. 2005; Kouzmanov and Pokrovski 2012; Seward et al. 2014; Zhong et al. 2015; Shu et al. 2017; Korges et al. 2019). Thermodynamic modelling performed by Zhong et al. (2015) at 1–5 kbar and 50–650 °C shows that Cu, Pb and Zn concentrations are strongly dependent on the redox-state, temperature and salinity of the fluid. However, magmatic systems are very different from basinal and metamorphic settings and more fluid data from the latter systems are clearly needed, in particular for systems that are mineralized in Pb and Zn. We suggest that fluid percolating through, and interacting with pre-existing stratabound epigenetic Zn-rich orebodies, hosted within high-grade metamorphic rock at lower crustal levels, may lead to significant enrichment in metal content in the fluid phases (dissolved and/or in solids). Stratabound orebodies are widespread in the Pyrenees and have been significantly exploited in the past, more so than the deposits related to crosscutting veins. (e.g., Pierrefitte, Bentaillou; Pouit 1978; Pouit and Bois 1986). Thus, the early stratabound epigenetic mineralization could represent an important metal source for the enrichment of fluids, represented by FIs in population (I) and (II), leading to an increased metal precipitation in the veins. Studies of the lead isotopic compositions in Pyrenean galena generally indicate a single metal source for the different mineralization styles, which aligns with our hypothesis (García-Sanseguendo et al. 2014; Cugerone et al. 2021b). In the literature, metamorphic terranes and Pb-Zn pre-enriched metasediments are often interpreted as potential source for metals and ore-deposit (e.g., the Mt. Lofty Ranges, South Australia; Hammerli et al. 2015). In these settings, metamorphic minerals such as biotite may serve as a source for base metals (Kunz et al. 2022). Although no study has specifically linked metamorphism to base metal formation in the Pyrenees, we frequently observed that high-grade metamorphic schists near Victoria contain metamorphic minerals rich in Zn, such as gahnite (Cugerone et al. 2018b). Crystalline rocks are also typically considered as a probable source for base metals, even for low-medium temperature (<300 °C) vein-style mineralization (Frape et al. 2003; Burisch et al.

2016a). In the Pyrenees, numerous Variscan calc-alkaline magmatic stocks are found near mineralized veins. However, the significant metal enrichment (Pb, Zn) observed in metasedimentary rocks, associated with stratabound epigenetic Pb-Zn ore bodies across the PAZ (Cugerone et al. 2018b), suggests a direct potential source for metal leaching into these crosscutting veins.

## Conclusion

In the Pyrenean Pb-Zn deposits, two types of fluids with distinct FI population types, salinity, temperatures, Ca-Sr and halogen concentrations are identified. Population (I) is CO<sub>2</sub>-rich with a low to medium salinity and high temperature (250–350 °C), is Na-dominated with poor Ca content, and has a homogeneous Cl/Br ratio with rather low values. Population (II) shows a medium to high salinity and lower temperature (<200 °C), is Ca-dominated and has a high Cl/Br ratio in average, although, significant variations suggest fluid mixing. Comparison with other deposits from the region and globally indicates that the characteristics of population (I), i.e., low Cl/Br ratio, abundant CO<sub>2</sub>-bearing FIs and Na-dominated, are consistent with a metamorphic origin for the fluid. In contrast, the Ca-dominated system with fewer CO<sub>2</sub>-bearing FIs and higher Cl/Br ratio typifying population (II), most likely reflects a basinal fluid that interacted extensively with basement rocks, presumably during the Mesozoic or Alpine periods. In FIs from both population (I) and (II), Pb-Zn concentrations can reach up to 1–2 wt% Zn-Pb in high-grade metamorphic rocks and progressively decrease at shallower levels (lower metamorphic grades). Based on a compilation of data from metamorphic and basinal fluids, we propose a correlation between the metal content in the fluid and the metamorphic grade or crustal level of the host rock, which is inversely proportional to the Cl/Br ratio. In our samples, secondary FIs crosscutting deformed sphalerite locally contain high Ge concentrations which correlate with Pb and Tl, suggesting the formation of Ge-rich sulfosalts within the fluid. This indicates that Ge may have been remobilized from Ge-rich sphalerite during deformation. This study highlights the importance of pre-existing metal enrichment in the crust, such as found in stratabound bodies and metamorphic rocks for the formation of Pb-Zn vein mineralization in multistage orogens.

**Supplementary Information** The online version contains supplementary material available at <https://doi.org/10.1007/s00126-024-01329-5>.

**Acknowledgements** This study was funded through the French national program “Référentiel Géologique de France” of the French Geological Survey (Bureau de Recherches Géologiques et Minières; BRGM) and the CESSUR/INSU/CNRS program. BC acknowledges



the funding from the European Union's Horizon 2020 research and innovation program under grant agreement No 793978. We are grateful to Tobias Fusswinkel and the anonymous reviewer for their constructive feedback, and to David Banks and Karen Kelley for their editorial guidance. Special thanks go to David Banks for his constructive comments and assistance in refining the final versions of the manuscript. The authors also acknowledge the PHC Germaine de Staël funding secured by Alain Chauvet. We thank Emilien Oliot for his contribution to sampling, and Christophe Nevado and Doriane Delmas for preparing high-quality double-polished fluid inclusion sections.

**Funding** Open access funding provided by University of Geneva

## Declarations

**Conflict of interest** The authors declare no conflict of interest.

**Open Access** This article is licensed under a Creative Commons Attribution 4.0 International License, which permits use, sharing, adaptation, distribution and reproduction in any medium or format, as long as you give appropriate credit to the original author(s) and the source, provide a link to the Creative Commons licence, and indicate if changes were made. The images or other third party material in this article are included in the article's Creative Commons licence, unless indicated otherwise in a credit line to the material. If material is not included in the article's Creative Commons licence and your intended use is not permitted by statutory regulation or exceeds the permitted use, you will need to obtain permission directly from the copyright holder. To view a copy of this licence, visit <http://creativecommons.org/licenses/by/4.0/>.

## References

- Appold MS, Wenz ZJ (2011) Composition of ore fluid inclusions from the Viburnum Trend, Southeast Missouri district, United States: implications for transport and precipitation mechanisms. *Econ Geol* 106:55–78. <https://doi.org/10.2113/econgeo.106.1.55>
- Banks DA, Da Vies GR, Yardley BWD, McCaig AM, Grant NT (1991) The chemistry of brines from an Alpine thrust system in the Central Pyrenees: an application of fluid inclusion analysis to the study of fluid behaviour in orogenesis. *Geochim Cosmochim Acta* 55:1021–1030. [https://doi.org/10.1016/0016-7037\(91\)90160-7](https://doi.org/10.1016/0016-7037(91)90160-7)
- Banks DA, Green R, Cliff RA, Yardley BWD (2000) Chlorine isotopes in fluid inclusions: determination of the origins of salinity in magmatic fluids. *Geochim Cosmochim Acta* 64:1785–1789. [https://doi.org/10.1016/S0016-7037\(99\)00407-X](https://doi.org/10.1016/S0016-7037(99)00407-X)
- Bertauts M, Vezinet A, Janots E, Rossi M, Duhamel-achin I, Lach P, Lanari P, Alpes G, Savoie U, Blanc M, Eiffel UG (2024) Cenozoic pb – zn – ag mineralization in the Western Alps. *Geol XX* 1–5. <https://doi.org/10.1130/G51818.1/6251078/g51818.pdf>
- Bonev IK, Kouzmanov K (2002) Fluid inclusions in sphalerite as negative crystals: a case study. *Eur J Mineral* 14:607–620. <https://doi.org/10.1127/0935-1221/2002/0014-0607>
- Bons PD, Fusswinkel T, Gomez-Rivas E, Markl G, Wagner T, Walter B (2014) Fluid mixing from below in unconformity-related hydrothermal ore deposits. *Geology* 42:1035–1038. <https://doi.org/10.1130/G35708.1>
- Bouhlef S, Leach DL, Johnson CA, Marsh E, Salmi-Laouar S, Banks DA (2016) A salt diapir-related Mississippi Valley-type deposit: the Bou Jaber Pb-Zn-Ba-F deposit. fluid inclusion and isotope study, Tunisia
- Burisch M, Marks MAW, Nowak M, Markl G (2016a) The effect of temperature and cataclastic deformation on the composition of upper crustal fluids - an experimental approach. *Chem Geol* 433:24–35. <https://doi.org/10.1016/j.chemgeo.2016.03.031>
- Burisch M, Walter BF, Wälle M, Markl G (2016b) Tracing fluid migration pathways in the root zone below unconformity-related hydrothermal veins: insights from trace element systematics of individual fluid inclusions. *Chem Geol* 429:44–50. <https://doi.org/10.1016/j.chemgeo.2016.03.004>
- Burisch M, Markl G, Gutzmer J (2022) Breakup with benefits - hydrothermal mineral systems related to the disintegration of a supercontinent. *Earth Planet Sci Lett* 580:117373. <https://doi.org/10.1016/j.epsl.2022.117373>
- Castroviejo Bolibar R, Serrano FM (1983) Estructura y metalogenia del campo filoniano de cierco (Pb-Zn-Ag), en El Pirineo De Lérida. *Boletín Geológico Y Min* 1983:291–320
- Cathelineau M, Boiron M-C, Jakomulski H (2021) Triassic evaporites: a vast reservoir of brines mobilized successively during rifting and thrusting in the Pyrenees. *J Geol Soc Lond* 1–18. <https://doi.org/10.1144/jgs2020-259>
- Channer DMD, de Ronde CEJ, Spooner ETC (1997) The Cl-Br-I composition of 3.23 Ga modified seawater: implications for the geological evolution of ocean halide chemistry. *Earth Planet Sci Lett* 150:325–335
- Cochelin B, Chardon D, Denèle Y, Gumiaux C, Le Bayon B (2017) Vertical strain partitioning in hot Variscan crust: syn-convergence escape of the pyrenees in the Iberian-Armorican syntax. *Bull La Société géologique Fr* 188:39. <https://doi.org/10.1051/bsgf/2017206>
- Cugerone A, Cenki-Tok B, Chauvet A, Le Goff E, Bailly L, Alard O, Allard M (2018a) Relationships between the occurrence of accessory Ge-minerals and sphalerite in Variscan Pb-Zn deposits of the Bossost Anticlinorium, French Pyrenean Axial Zone: Chemistry, microstructures and ore-deposit setting. *Ore Geol Rev* 95:1–19. <https://doi.org/10.1016/j.oregeorev.2018.02.016>
- Cugerone A, Oliot E, Chauvet A, Gavaldà Bordes J, Laurent A, Le Goff E, Cenki-Tok B (2018b) Structural control on the formation of Pb-Zn deposits: an Example from the Pyrenean Axial Zone. *Minerals* 8:1–20. <https://doi.org/10.3390/min8110489>
- Cugerone A, Cenki-tok B, Oliot E, Muñoz M, Barou F, Motto-Ros V, Le Goff E (2020) Redistribution of germanium during dynamic recrystallization of sphalerite. *Geology* 48:236–241. <https://doi.org/10.1130/G46791.1>
- Cugerone A, Cenki-Tok B, Muñoz M, Kouzmanov K, Oliot E, Motto-Ros V, Le Goff E (2021a) Behavior of critical metals in metamorphosed Pb-Zn ore deposits: example from the Pyrenean Axial Zone. *Min Depos* 56. <https://doi.org/10.1007/s00126-020-01000-9>
- Cugerone A, Roger F, Cenki B, Oliot E, Paquette JL (2021b) Variscan U-Th-Pb age for stratabound Pb-Zn mineralization in the Bossost dome (Pyrenean Axial Zone). *Ore Geol Rev* 139, Part:1–18. <https://doi.org/10.1016/j.oregeorev.2021.104503>
- Cugerone A, Roger F, Cenki B, Oliot E, Paquette J-L (2022) Variscan U-th-pb age for stratabound Pb-Zn mineralization in the Bossost dome (Pyrenean Axial Zone). *Ore Geol Rev*
- Cugerone A, Oliot E, Munoz M, Barou F, Motto-Ros V, Cenki B (2024) Plastic deformation and trace element mobility in sphalerite. *Am Mineral* 1–68
- Dewaele S, Muchez P, Banks DA (2004) Fluid evolution along multistage composite fault systems at the southern margin of the Lower Palaeozoic Anglo-Brabant fold belt. *Belgium Geofluids* 4:341–356. <https://doi.org/10.1111/j.1468-8123.2004.00096.x>
- Fall A, Bodnar RJ (2018) How precisely can the temperature of a fluid event be constrained using fluid inclusions? *Econ Geol* 113:1817–1843. <https://doi.org/10.5382/econgeo.2018.4614>
- Fanlo I, Touray JC, Subías I, Fernández-Nieto C (1998) Geochemical patterns of a sheared fluorite vein, Parzan, Spanish central

- Pyrenees. *Min Depos* 33:620–632. <https://doi.org/10.1007/s001260050177>
- Fontboté L, Kouzmanov K, Chiaradia M, Pokrovski GS (2017) Sulfide minerals in hydrothermal deposits. *Elements* 13:97–103. <https://doi.org/10.2113/gselements.13.2.97>
- Fougereuse D, Cugerone A, Reddy SM, Luo K, Motto-ros V (2023) Nanoscale distribution of Ge in Cu-rich sphalerite. *Geochim Cosmochim Acta* 346:223–230. <https://doi.org/10.1016/j.gca.2023.02.011>
- Frape SK, Blyth A, Blomqvist R, McNutt RH, Gascoyne M (2003) Deep fluids in the continents: II. Crystalline rocks. *Treatise Geochem* 5–9:541–580. <https://doi.org/10.1016/B0-08-043751-6/05086-6>
- Fusswinkel T, Wagner T, Wälle M, Wenzel T, Heinrich CA, Markl G (2013) Fluid mixing forms basement-hosted Pb-Zn deposits: insight from metal and halogen geochemistry of individual fluid inclusions. *Geology* 41:679–682. <https://doi.org/10.1130/G34092.1>
- Fusswinkel T, Wagner T, Sakellaris G (2017) Fluid evolution of the Neoproterozoic Pampalo orogenic gold deposit (E Finland): constraints from LA-ICPMS fluid inclusion microanalysis. *Chem Geol* 450:96–121. <https://doi.org/10.1016/j.chemgeo.2016.12.022>
- Fusswinkel T, Giehl C, Beermann O, Fredriksson JR, Garbe-Schönberg D, Scholten L, Wagner T (2018) Combined LA-ICP-MS microanalysis of iodine, bromine and chlorine in fluid inclusions. *J Anal Spectrom* 33:768–783. <https://doi.org/10.1039/c7ja00415j>
- Fusswinkel T, Niinikoski-Fusswinkel P, Wagner T (2022) Halogen ratios in crustal fluids through time—proxies for the emergence of aerobic life? *Geology* 50:1096–1100. <https://doi.org/10.1130/G50182.1>
- García-Sanssegundo J, Alonso JL (1989) Stratigraphy and structure of the southeastern Garona Dome. *Geodin Acta* 3:127–134. <https://doi.org/10.1080/09853111.1989.11105180>
- García-Sanssegundo J, Martín-Izard A, Gavalà J (2014) Structural control and geological significance of the Zn-Pb ores formed in the Benasque Pass area (Central Pyrenees) during the post-late ordo-vician extensional event of the Gondwana margin. *Ore Geol Rev* 56:516–527. <https://doi.org/10.1016/j.oregeorev.2013.06.001>
- Giorno M, Barale L, Bertok C, Frenzel M, Looser N, Guillong M, Bernasconi SM, Martire L (2022) Sulfide-associated hydrothermal dolomite and calcite reveal a shallow burial depth for Alpine-type Zn-(Pb) deposits. *Geology* 50:853–858. <https://doi.org/10.1130/G49812.1>
- Goldstein RH (1994) Chap. 2: Petrographic Analysis of Fluid Inclusions. *Mineral Assoc Canada*, pp 1–43
- Goldstein RH, Reynolds TJ (1994) Systematics of fluid inclusions in Diagenetic Minerals. *SEPM Short Course* 31:1–213
- Grandia F, Canals À, Cardellach E, Banks DA, Perona J (2003a) Origin of ore-forming brines in sediment-hosted Zn-Pb deposits of the basque-cantabrian basin, Northern Spain. *Econ Geol* 98:1397–1411. <https://doi.org/10.2113/gsecongeo.98.7.1397>
- Grandia F, Cardellach E, Canals À, Banks DA (2003b) Geochemistry of the fluids related to epigenetic carbonate-hosted Zn-Pb deposits in the Maestrat basin, Eastern Spain: fluid inclusion and isotope (Cl, C, O, S, Sr) evidence. *Econ Geol* 98:933–954. <https://doi.org/10.2113/gsecongeo.98.5.933>
- Guilcher M, Albert R, Gerdes A, Gutzmer J, Burisch M (2021) Timing of native metal-arsenide (Ag-Bi-Co-Ni-As ± U) veins in continental rift zones – in situ U-Pb geochronology of carbonates from the Erzgebirge/Krušné Hory province. *Chem Geol* 584:120476. <https://doi.org/10.1016/j.chemgeo.2021.120476>
- Guillong M, Heinrich CA (2007) Sensitivity enhancement in laser ablation ICP-MS using small amounts of hydrogen in the carrier gas. *J Anal Spectrom* 22:1488–1494. <https://doi.org/10.1039/b709489b>
- Guillong M, Meier DL, Allan MM, Heinrich CA, Yardley BWD (2008) SILLS: a Matlab-based program for the reduction of laser ablation ICP-MS data of homogeneous materials and inclusions. *Mineral Assoc Can Short Course* 40:328–333
- Hammerli J, Spandler C, Oliver NHS, Sossi P, Dipple GM Zn and Pb mobility during metamorphism of sedimentary rocks and potential implications for some base metal deposits Hammerli, Spandler J, Oliver C, Sossi NHS, Dipple P (2015) G.M., 2015. Zn and Pb mobility during metamorphism of sedimentary rocks and p. *Miner Depos* 50:657–664. <https://doi.org/10.1007/s00126-015-0600-5>
- Heijlen W, Banks DA, Muchez P, Stensgard BM, Yardley BWD (2008) The nature of mineralizing fluids of the Kipushi Zn-Cu deposit, Katanga, Democratic Republic of Congo: quantitative fluid inclusion analysis using laser ablation ICP-MS and bulk crush-leach methods. *Econ Geol* 103:1459–1482. <https://doi.org/10.2113/gsecongeo.103.7.1459>
- Jochum KP, Weis U, Stoll B, Kuzmin D, Yang Q, Raczek I, Jacob DE, Stracke A, Birbaum K, Frick DA, Günther D, Enzweiler J (2011) Determination of reference values for NIST SRM 610–617 glasses following ISO guidelines. *Geostand Geoanalytical Res* 35:397–429. <https://doi.org/10.1111/j.1751-908X.2011.00120.x>
- Johnson CA, Cardellach E, Tritlla J, Hanan BB (1996) Cierco Pb-Zn-Ag Vein deposits: isotopic and fluid inclusion evidence for formation during the mesozoic extension in the pyrenees of Spain. *Econ Geol* 91:497–506. <https://doi.org/10.5962/bhl.title.18736>
- Kesler SE, Richard Kyle J, Appold MS, Huston TJ, Walter LM, Martini AM (1995) Na-Cl-Br systematics of mineralizing brines in Mississippi Valley-type deposits. *Geology* 23:641–644. [https://doi.org/10.1130/0091-7613\(1995\)023<0641:nbsom>2.3.co;2](https://doi.org/10.1130/0091-7613(1995)023<0641:nbsom>2.3.co;2)
- Korges M, Weis P, Lüders V, Laurent O (2019) Sequential evolution of Sn–Zn–In mineralization at the skarn-hosted Hämmerlein deposit, Erzgebirge, Germany, from fluid inclusions in ore and gangue minerals. *Min Depos* 1–16
- Kouzmanov K, Pokrovski GS (2012) Hydrothermal Controls on Metal Distribution in Porphyry Cu-(Mo-Au) systems. *SEG Spec Publ* 16:573–618
- Kunz BE, Warren CJ, Jenner FE, Harris NBW, Argles TW (2022) Critical metal enrichment in crustal melts: the role of metamorphic mica. *Geology* 50:1219–1223. <https://doi.org/10.1130/g50284.1>
- Landtwing MR, Pettke T, Halter WE, Heinrich CA, Redmond PB, Einaudi MT, Kunze K (2005) Copper deposition during quartz dissolution by cooling magmatic-hydrothermal fluids: the Bingham porphyry. *Earth Planet Sci Lett* 235:229–243. <https://doi.org/10.1016/j.epsl.2005.02.046>
- Laznicka P (2006) Giant metallic deposits: future sources of industrial metals. *Springer* 1–732. <https://doi.org/10.1007/3-540-33092-5>
- Leach DL, Rowan EL (1986) Genetic link between Ouachita foldbelt tectonism and the Mississippi Valley-type lead-zinc deposits of the ozarks (USA). *Geology* 14:931–935. [https://doi.org/10.1130/0091-7613\(1986\)14<931:GLBOFT>2.0.CO;2](https://doi.org/10.1130/0091-7613(1986)14<931:GLBOFT>2.0.CO;2)
- Leach DL, Macquar JC, Lagneau V, Leventhal JS, Emsbo P, Premo W (2006) Precipitation of lead-zinc ores in the Mississippi Valley type deposit at Treves, cevennes region of southern France. *Geofluids* 6:24–44. <https://doi.org/10.1111/j.1468-8123.2006.00126.x>
- Luo K, Cugerone A, Zhou M-F, Zhou J-X, Sun G-T, Xu J, He K-J, Lu M-D (2022) Germanium enrichment in sphalerite with acicular and euhedral textures: an example from the Zhulingou carbonate-hosted Zn-(Ge) deposit, South China. *Min Depos*. <https://doi.org/10.1007/s00126-022-01112-4>
- Marsala A, Wagner T, Wälle M (2013) Late-metamorphic veins record deep ingressions of meteoric water: a LA-ICPMS fluid inclusion study from the fold-and-thrust belt of the Rhenish Massif, Germany. *Chem Geol* 351:134–153. <https://doi.org/10.1016/j.chemgeo.2013.05.008>
- McCaig AM, Tritlla J, Banks DA (2000) Fluid flow patterns during Pyrenean thrusting. *J Geochemical Explor* 70:539–543

- Mezger JE, Passchier CW (2003) Polymetamorphism and ductile deformation of staurolite–cordierite schist of the Bossòst dome: indication for Variscan extension in the Axial Zone of the central Pyrenees. *Geol Mag* 140:595–612. <https://doi.org/10.1017/S0016756803008112>
- Miron GD, Wagner T, Wälle M, Heinrich CA (2013) Major and trace-element composition and pressure–temperature evolution of rock-buffered fluids in low-grade accretionary-wedge metasediments, Central Alps. *Contrib Mineral Petrol* 165:981–1008. <https://doi.org/10.1007/s00410-012-0844-3>
- Mu L, Hu R, Bi X, Tang Y, Lan T, Lan Q, Zhu J (2021) New insights into the origin of the World-Class Jinding Sediment-Hosted Zn–Pb Deposit, Southwestern China: evidence from LA-ICP-MS analysis of individual fluid inclusions. *Econ Geol*. <https://doi.org/10.5382/econgeo.4826>
- Muche P, Heijlen W, Banks D, Blundell D, Boni M, Grandia F (2005) 7: Extensional tectonics and the timing and formation of basin-hosted deposits in Europe. *Ore Geol Rev* 27:241–267. <https://doi.org/10.1016/j.oregeorev.2005.07.013>
- Müller A, Ehle H (2021) Rapid ore classification for real-time mineral processing optimisation at the Niederschlag multi-generation hydrothermal barite-fluorite vein deposit, Germany. *Min Depos* 56:417–424. <https://doi.org/10.1007/s00126-020-01037-w>
- Munoz M, Boyce AJ, Courjault-Rade P, Fallick AE, Tollon F (1994) Multi-stage fluid incursion in the palaeozoic basement-hosted Saint-Salvy ore deposit (NW Montagne Noire, southern France). *Appl Geochem* 9:609–626. [https://doi.org/10.1016/0883-2927\(94\)90022-1](https://doi.org/10.1016/0883-2927(94)90022-1)
- Munoz M, Boyce A, Courjault-Rade P, Fallick A, Tollon F (1997) Le Filon (Zn, F) de peyrebrune (SW Massif central, France): caractérisation géochimique Des fluides Au Cours Du Mésozoïque à La Bordure Orientale Du Bassin d'Aquitaine. *Compte Rendu Acad Sci Paris t* 324:899–906
- Munoz M, Baron S, Boucher A, Béziat D, Salvi S (2016) Mesozoic vein-type Pb–Zn mineralization in the Pyrenees: lead isotopic and fluid inclusion evidence from the Les Argentières and Lacore deposits. *Comptes Rendus Geosci* 348:322–332. <https://doi.org/10.1016/j.crte.2015.07.001>
- Neuser RD (1995) A new high-intensity cathodoluminescence microscope and its application to weakly luminescing minerals. *Bochum Geol Und Geotech Arb* 44:116–118
- Oliver J (1986) Fluids expelled tectonically from orogenic belts: their role in hydrocarbon migration and other geologic phenomena. *Geology* 14:99–102. [https://doi.org/10.1130/0091-7613\(1986\)14<99:FETF0B>2.0.CO;2](https://doi.org/10.1130/0091-7613(1986)14<99:FETF0B>2.0.CO;2)
- Pouit G (1978) Différents Modeles De Mineralisations «Hydrothermale Sédimentaire», à Zn (Pb) Du Paléozoïque Des Pyrénées Centrales. *Min Depos* 13:411–421
- Pouit G (1985) Les minéralisations Zn (Pb) Ba Du Paléozoïque Des Pyrénées Centrales: Une Mise Au point et un compte rendu des missions 1984. *Bur Rech Géologiques Minières Rapp* 85 DAM037:72
- Pouit G, Bois JP (1986) Arrens Zn (Pb), Ba Devonian deposit, Pyrénées, France: an exhalative-sedimentary-type deposit similar to Meggen. *Min Depos* 21:181–189
- Quesnel B, Boiron M-C, Cathelineau M, Truche L, Rigaudier T, Bardoux G, Agrinier P, de Saint Blanquat M, Masini E, Gaucher EC (2019) Nature and Origin of mineralizing fluids in Hyperextensional systems: the case of cretaceous mg metasomatism in the Pyrenees. *Geofluids* 2019:1–18. <https://doi.org/10.1155/2019/7213050>
- Rauchenstein-Martinek K, Wagner T, Wälle M, Heinrich CA (2014) Gold concentrations in metamorphic fluids: a LA-ICPMS study of fluid inclusions from the Alpine orogenic belt. *Chem Geol* 385:70–83. <https://doi.org/10.1016/j.chemgeo.2014.07.018>
- Rauchenstein-Martinek K, Wagner T, Wälle M, Heinrich CA, Arlt T (2016) Chemical evolution of metamorphic fluids in the Central Alps, Switzerland: insight from LA-ICP-MS analysis of fluid inclusions. *Geofluids* 16:877–908. <https://doi.org/10.1111/gfl.12194>
- Reyx J (1973) Relations entre tectonique, métamorphisme de contact et concentrations métalliques dans le secteur des anciennes mines d'Arre et Anglas (Hautes-Pyrénées - Pyrénées atlantiques). Ph D Thesis, Univ Paris VI 83p
- Roedder E (1984) Fluid inclusions. *Mineral Soc Am* 646p
- Scharrer M, Fusswinkel T, Markl G (2023) Triple-halogen (Cl–Br–I) fluid inclusion LA-ICP-MS microanalysis to unravel iodine behavior and sources during marine fluid infiltration into the basement in unconformity settings. *Geochim Cosmochim Acta* 357:64–76. <https://doi.org/10.1016/j.gca.2023.06.023>
- Schlöglöva K, Wälle M, Heinrich CA (2017) LA-ICP-MS analysis of fluid inclusions: contamination effects challenging micro-analysis of elements close to their detection limit. *J Anal Spectrom* 32:1052–1063. <https://doi.org/10.1039/c7ja00022g>
- Seo JH, Guillion M, Aerts M, Zajacz Z, Heinrich CA (2011) Microanalysis of S, Cl, and Br in fluid inclusions by LA-ICP-MS. *Chem Geol* 284:35–44. <https://doi.org/10.1016/j.chemgeo.2011.02.003>
- Seward TM, Williams-Jones AE, Migdisov AA (2014) *The Chemistry of Metal Transport and Deposition by Ore-Forming Hydrothermal fluids*, 2nd edn. Elsevier Ltd
- Shu Q, Chang Z, Hammerli J, Lai Y, Huizenga JM (2017) Composition and evolution of fluids forming the Baiyinnuo'er Zn–Pb Skarn deposit, northeastern China: insights from laser ablation ICP-MS study of fluid inclusions. *Econ Geol* 112:1441–1460. <https://doi.org/10.5382/econgeo.2017.4516>
- Song Y, Hou Z, Liu Y, Zhuang L, Hu G (2023) Mississippi Valley-type Zn–Pb deposits in orogenic thrust belts: ore formation in response to synorogenic crustal transpression or extension. *Min Depos* 58:1333–1350. <https://doi.org/10.1007/s00126-023-01185-9>
- Sośnicka M, Lüders V, Duschl F, Kraemer D, Laurent O, Niedermann S, Banks DA, Wilke F, Wohlgemuth-Ueberwasser C, Wiedenbeck M (2023) Metal budget and origin of aqueous brines depositing deep-seated Zn–Pb mineralization linked to hydrocarbon reservoirs, North German Basin. *Miner Depos*. <https://doi.org/10.1007/s00126-023-01173-z>
- Steele-MacInnis M (2018) Fluid inclusions in the system H<sub>2</sub>O–NaCl–CO<sub>2</sub>: an algorithm to determine composition, density and isochore. *Chem Geol* 498:31–44. <https://doi.org/10.1016/j.chemgeo.2018.08.022>
- Steele-MacInnis M, Bodnar RJ, Naden J (2011) Numerical model to determine the composition of H<sub>2</sub>O–NaCl–CaCl<sub>2</sub> fluid inclusions based on microthermometric and microanalytical data. *Geochimica Cosmochim Acta* 75:21–40. <https://doi.org/10.1016/j.gca.2010.10.002>
- Steele-MacInnis M, Lecumberri-Sanchez P, Bodnar RJ (2012) HokieFlinCS\_H<sub>2</sub>O–NaCl: a Microsoft Excel spreadsheet for interpreting microthermometric data from fluid inclusions based on the PVTX properties of H<sub>2</sub>O–NaCl. *Comput Geosci* 49:334–337. <https://doi.org/10.1016/j.cageo.2012.01.022>
- Stoffell B, Appold MS, Wilkinson JJ, McClean NA, Jeffries TE (2008) Geochemistry and evolution of mississippi valley-type mineralizing brines from the Tri-state and Northern Arkansas districts determined by LA-ICP-MS microanalysis of fluid inclusions. *Econ Geol* 103:1411–1435. <https://doi.org/10.2113/gsecongeo.103.7.1411>
- Subias I, Fanlo I, Yuste A, Fernandez-Nieto C (1999) The Yenefrito Pb–Zn mine (Spanish Central Pyrenees): an example of superimposed metallogenetic events. *Min Depos* 34:220–223
- Sun G, Zhou J, Cugerone A, Zhou M, Zhou L (2023) Germanium-rich nanoparticles in Cu-poor sphalerite: a new mechanism for



- Ge enrichment. GSA Bull 1–15. <https://doi.org/10.1130/B37014.1/6040167/b37014.pdf>
- Tomkins AG (2007) Three mechanisms of ore re-mobilisation during amphibolite facies metamorphism at the Montauban Zn-Pb-Au-Ag deposit. *Min Depos* 42:627–637. <https://doi.org/10.1007/s00126-007-0131-9>
- Vergés J, Fernández M, Martínez A (2002) The Pyrenean orogen: Pre-, syn-, and post-collisional evolution. *J Virtual Explor* 8:1–20. <https://doi.org/10.3809/jvirtex.2002.00058>
- Walter LM, Stueber AM, Huston TJ (1990) Br-Cl-Na systematics in Illinois basin fluids: constraints on fluid origin and evolution. *Geology* 18:315–318. [https://doi.org/10.1130/0091-7613\(1990\)018<0315:BCNSII>2.3.CO;2](https://doi.org/10.1130/0091-7613(1990)018<0315:BCNSII>2.3.CO;2)
- Wilkinson JJ (2013) Sediment-Hosted Zinc-Lead Mineralization: Processes and Perspectives: Processes and Perspectives, Treatise on Geochemistry, Second Edition. Elsevier, H Holland, K Turekian (ed), Amsterdam, Netherlands 219–249. <https://doi.org/10.1016/B978-0-08-095975-7.01109-8>
- Wilkinson JJ, Stoffell B, Wilkinson CC, Jeffries TE, Appold MS (2009) Anomalously metal-rich fluids form hydrothermal ore deposits. *Sci (80-)* 323:764–767. <https://doi.org/10.1126/science.1164436>
- Yardley BWD (2005) Metal concentrations in Crustal fluids and their relationship to Ore formation. *Econ Geol* 100:613–632
- Yardley BWD, Bodnar RJ (2014) Fluids in the continental crust. *Geochemical Perspect* 3:1–127. <https://doi.org/10.7185/geochempers.p.3.1>
- Yardley BWD, Cleverley JS (2015) The role of metamorphic fluids in the formation of ore deposits. *Geol Soc Lond Spec Publ* 393:117–134. <https://doi.org/10.1144/sp393.5>
- Zhong R, Brugger J, Chen Y, Li W (2015) Contrasting regimes of Cu, Zn and Pb transport in ore-forming hydrothermal fluids. *Chem Geol* 395:154–164. <https://doi.org/10.1016/j.chemgeo.2014.12.008>
- Zwart HJ (1963) Metamorphic history of the Central Pyrenees, Part II, Valle De Aran. *Leidse Geol Meded* 28:321–376
- Zwart HJ (1979) The geology of the Central Pyrenees. *Leidse Geol Meded* 50:1–74

**Publisher's note** Springer Nature remains neutral with regard to jurisdictional claims in published maps and institutional affiliations.